J. Fluid Mech. (2014), *vol.* 750, *pp.* 210–244. © Cambridge University Press 2014
doi:10.1017/jfm.2014.246

Two-dimensional planar plumes and fountains

T. S. van den Bremer[1,†] and G. R. Hunt[2,†]

[1]Department of Engineering Science, University of Oxford, Parks Road, Oxford OX1 3PJ, UK

[2]Department of Engineering, University of Cambridge, Trumpington Street, Cambridge CB2 1PZ, UK

(Received 18 February 2013; revised 11 February 2014; accepted 30 April 2014;
first published online 4 June 2014)

Closed-form solutions describing the behaviour of two-dimensional planar turbulent rising plumes and fountains from horizontal planar area and line sources in unconfined quiescent environments of uniform density are proposed. Extending the analysis on axisymmetric releases by van den Bremer & Hunt (*J. Fluid Mech.*, vol. 644, 2010, pp. 165–192) to planar releases, the local flux balance parameter $\Gamma = \Gamma(z)$ is instrumental in describing the bulk behaviour of steady Boussinesq and non-Boussinesq planar plumes and the initial rise behaviour of Boussinesq planar fountains as a function of height z. Expressions for the asymptotic virtual source correction are developed and the results elucidated by 'scale diagrams' (cf. Morton & Middleton, *J. Fluid Mech.*, vol. 58, 1973, pp. 165–176) showing certain characteristic heights for different source conditions. These diagrams capture all the different manifestations of plume behaviour, encompassing fountains, jets, source-momentum-dominated or 'forced' plumes, pure plumes and source-buoyancy-dominated or 'lazy' plumes, and their associated key features. Other flow features identified include a gravity-driven deceleration regime and a mixing-driven regime for forced fountains. Deceleration in lazy fountains is purely gravity-driven. The results can be shown to be valid for both Boussinesq and non-Boussinesq plumes (but not for non-Boussinesq fountains) thus resulting in universal solutions valid for both cases provided the entrainment velocity is unaffected by non-Boussinesq effects. This paper presents and explores these universal solutions. An accompanying paper (van den Bremer & Hunt, *J. Fluid Mech.*, vol. 750, 2014, pp. 245–258) examines the implications for non-Boussinesq plumes. The existing solutions of Lee & Emmons (*J. Fluid Mech.*, vol. 11, 1961, pp. 353–368) generalized herein are valid for a constant entrainment coefficient α. New results for an entrainment coefficient that varies linearly with $\Gamma(z)$ and thus captures experimental values far more realistically are presented for forced plumes.

Key words: convection, plumes/thermals

1. Introduction

Turbulent planar plumes arising from horizontal area sources have received significantly less attention than axisymmetric plumes. This is especially evident for non-Boussinesq planar plumes for which experimental studies appear entirely absent from the literature. Notwithstanding, planar plumes occur in a wide variety of

† Email addresses for correspondence: ton.vandenbremer@eng.ox.ac.uk, gary.hunt@eng.cam.ac.uk

https://doi.org/10.1017/jfm.2014.246 Published online by Cambridge University Press

circumstances both in the natural and the man-made environments. The saline plumes that form at leads in melting sea ice (Wettlaufer, Worster & Huppert 1997; Widell, Fer & Haugan 2006), where cracks in the ice expose salt water to the atmosphere and evaporation drives off fresh water resulting in regions of locally higher salinity driving convection, are planar in nature. Pollutants are often discharged into the ocean through planar diffusers (Koh & Brooks 1975; Jirka 2006). Domestic and industrial ventilation provide other examples of planar sources from which plumes (e.g. from chilled beams) or fountains (e.g. from air curtains at doorways) form. Moreover, a row of closely spaced axisymmetric sources is often better modelled as one planar source, for example a row of audience members in a crowded lecture theatre (Radomski 2008). In the laboratory, truly planar plumes are notoriously difficult to create owing to practical challenges in achieving uniform source conditions along the entire length of the source. Crucially, we are interested in plumes that are not only planar but are in fact two-dimensional in nature, that is, for which the horizontal length of the source L is large relative to the source half-width of the plume b_0 ($L \gg b_0$), a simplifying assumption that is commonly made in the literature. This geometry is typical of ice leads which may extend tens of kilometres with widths of only $O(10)$–$O(100)$ m (Ching, Fernando & Noh 1993). Despite the two-dimensional nature of the source, turbulent eddies responsible for the entrainment of ambient fluid into the plume or fountain are fundamentally three-dimensional and the time-dependent turbulent properties of the fluid vary both across and along the main axis of the plume. By focusing our attention on quantities that are averaged both in time and in the along-axis direction, we achieve turbulence closure based on these double averages. All the quantities considered are thus averaged in time and along the axis of the plume.

The behaviour of Boussinesq turbulent buoyant plumes rising from horizontal long planar sources in unconfined quiescent environments of uniform density was first studied by Rouse, Yih & Humphreys (1952). They derived functional relationships for the key variables based on similarity considerations and combined these with the results from their experiments. Rouse *et al.* (1952) establish power-law solutions valid for pure plumes with generic cross-stream profiles. Additionally, they show that measurements of the vertical velocity and the effective gravity, when suitably scaled, each fall onto one bell-shaped curve and thereby confirm their self-similarity hypothesis. Their work was followed by a more systematic attempt to model the behaviour of planar plumes across a range of source Richardson numbers by Lee & Emmons (1961), whose approach is analogous to that of Morton, Taylor & Turner (1956) and Morton (1959) for axisymmetric plumes. Lee & Emmons (1961) assume that the plume is Boussinesq and thin so that pressure variations in the vertical direction are small and can be ignored (their 'boundary layer' assumption), and they adopt the entrainment model proposed by Taylor (1945) and subsequently adopted by Morton *et al.* (1956) to achieve turbulence closure. Assuming steadiness in time, the system of partial differential equations describing the flow was then transformed into a system of ordinary differential equations describing the behaviour of the fluxes of momentum, buoyancy and mass or volume. The development of these so-called plume conservation equations, which will be used as the starting point of the discussion herein, has recently been re-examined in a review of the historical development of classical plume theory by van den Bremer & Hunt (2010). Notably, when applying plume theory, the practitioner is faced with classifying the plume in question as Boussinesq, or non-Boussinesq when the density difference between the plume and ambient fluid is significant relative to the latter's density. The Boussinesq approximation thence amounts to ignoring such density differences, when they are small, except where they are responsible for the existence of a buoyancy force.

https://doi.org/10.1017/jfm.2014.246 Published online by Cambridge University Press

The famous entrainment model of Taylor (1945) assumes that the horizontal entrainment velocity u_e is proportional to the local vertical velocity w of the plume with a constant of proportionality α, referred to as the entrainment coefficient. In their experimental study, Kotsovinos & List (1977) argued for an improved description of entrainment, implementing the hypothesis of Priestley & Ball (1955), namely that α is a linear function of the local Richardson number. Delichatsios (1988), with further clarification by Thomas & Delichatsios (2007), concludes from similarity arguments that the entrainment model $u_e = \alpha w$ applies to both Boussinesq and non-Boussinesq planar plumes with one universal entrainment coefficient α that, unlike axisymmetric plumes, does not depend on the local density contrast. Although the solutions presented herein with such an entrainment assumption are universally valid for Boussinesq and non-Boussinesq plumes, the implications of this assumption and its validity are explored in an accompanying paper (van den Bremer & Hunt 2014).

The different types of solution (§ 3) to the conservation equations for planar plumes can be classified according to the source flux balance parameter, which arises naturally on non-dimensionalizing the plume conservation equations, defined here for the Boussinesq case with top-hat profiles (§ 2.2) by:

$$\Gamma_0 = \frac{B_0 Q_0^3}{2\alpha M_{B,0}^3}. \tag{1.1}$$

Here, B_0 denotes the source buoyancy flux per unit length (dimensions L^3T^{-3}), Q_0 the source volume flux per unit length (L^2T^{-1}) and $M_{B,0}$ the source momentum flux per unit length (L^3T^{-2}) under the Boussinesq approximation. Without approximation, the source momentum flux per unit length is M_0 (L^3T^{-2}). As for all the relevant quantities in this paper, the fluxes are averaged in time and in the direction along the axis of symmetry of the plume and have been normalized by the (uniform) ambient density ρ_a, where appropriate. The source parameter (1.1) can also be defined as the ratio of two length scales, a jet length L_J and a source length L_S, which we define as:

$$L_J \equiv \frac{\alpha^{2/3} M_{B,0}}{2^{1/3} B_0^{2/3}}, \quad L_S \equiv \frac{Q_0^2}{2M_{B,0}}, \quad \Gamma_0 = \left(\frac{L_S}{L_J}\right)^{3/2}, \tag{1.2a–c}$$

where $L_S = b_0$, b_0 denoting the source half-width of the plume, i.e. at $z = 0$. Note that the coefficients in (1.1) and (1.2) have been chosen for consistency with top-hat profiles (§§ 2.2 and 2.4).

As for axisymmetric releases (van den Bremer & Hunt 2010), five classes of solution to the planar conservation equations can be established: fountains ($\Gamma_0 < 0$) with source fluxes of buoyancy and momentum acting in opposing directions ($B_0 M_0 < 0$), pure jets ($\Gamma_0 = 0$) with zero source buoyancy flux, forced plumes ($0 < \Gamma_0 < 1$) dominated by their source momentum flux for heights up to the order of a jet length, pure plumes ($\Gamma_0 = 1$) with the source fluxes exactly in balance, and lazy plumes ($\Gamma_0 > 1$), which may be regarded as having a deficit of source momentum flux or, alternatively, an excess of mass flux (non-Boussinesq case) or volume flux (Boussinesq case) at the source compared with a pure plume. A single source parameter gives a unique representation of the behaviour that can be observed for steady releases and enables a characterization of the different types of bulk behaviour of rising plumes and fountains from general area sources. For axisymmetric releases, Morton (1959) solved the conservation equations for fountains and for forced and lazy plumes. By applying an asymptotic virtual source correction as a vertical origin

https://doi.org/10.1017/jfm.2014.246 Published online by Cambridge University Press

offset, Morton (1959) showed that the solutions for plumes rising from area sources can be replaced by the much simpler power-law solutions for plumes rising from point sources, the power-law solutions matching the original solution in the far field.

To solve the system of planar plume conservation equations Hunt & Coffey (2009), who study planar fountains, have adopted the Γ-centred approach proposed by Hunt & Kaye (2005), which is equivalent to the approach adopted herein. In this approach the parameter $\Gamma(z)$, where $z = 0$ denotes the location of the actual source, is defined as a local Richardson number expressed in terms of the local fluxes: $\Gamma(z) = B(z)Q^3(z)/2\alpha M_B^3(z)$. The bulk plume and fountain behaviours at any height are captured through the parameter Γ; hence solving for $\Gamma(z)$ immediately reveals the plume or fountain behaviour with height z. Using this Γ-centred approach, van den Bremer & Hunt (2010) obtained closed-form solutions that are universally applicable to Boussinesq and non-Boussinesq axisymmetric plumes.

Modifications to the plume conservation equations, focusing on axisymmetric releases, have been numerous and diverse. Such modifications include a time-dependent implementation (Scase *et al.* 2006) and inclusion of an internal mechanism for changing buoyancy through chemical reaction (Conroy & Llewellyn Smith 2008; Campbell & Cardoso 2010). For a review of the different aspects of turbulent plumes, including applications and development of different theories, the reader is referred to Turner (1966), Linden (2000), Kaye (2008), Woods (2010) and Hunt & van den Bremer (2011). For planar plumes in particular, Kay (2007) modified the conservation equations to allow for a quadratic dependence of density on temperature. Hunt & Coffey (2009) applied the conservation equations to planar fountains and did so using the aforementioned Γ-centred approach. For the axisymmetric case, Mehaddi, Vauquelin & Candelier (2012) also adopt the Γ-centred approach to propose closed-form solutions for fountains in stratified environments. In an experimental study, Bush & Woods (1999) consider planar plumes in a geophysical context by placing long linear sources in a rotating ambient and examine the formation of vortical structures that arise.

The majority of advances in plume theory have focused on axisymmetric plumes, with application to planar plumes being left aside after the seminal paper of Lee & Emmons (1961). Although many results for axisymmetric plumes can be readily extended to planar plumes, there are fundamental differences in behaviour between the two. This paper aims to bridge this gap in the literature. It explores solutions for plumes and fountains rising from planar sources by expressing the planar plume conservation equations in terms of the flux balance parameter Γ. Closed-form solutions to the system of conservation equations can then be readily obtained in a form that is instrumental in describing the key aspects of the behaviour of planar fountains and plumes.

This paper thereby clarifies and exposes the results of Lee & Emmons (1961). The behaviour of planar plumes and fountains is further elucidated by scale diagrams, analogous to the scale diagrams for axisymmetric Boussinesq plumes of Morton & Middleton (1973). These diagrams show different non-dimensional characteristic heights (including the asymptotic virtual source correction) as a function of the source conditions described by Γ_0. The behaviour of plumes and fountains is further clarified by exploring the variation of Γ, the density contrast and the relevant non-dimensional fluxes with height and doing so for different values of Γ_0. In addition, new solutions for an entrainment coefficient that varies linearly with the value of the local flux balance parameter Γ are presented for forced plumes leading to another class of solution, a class in which forced plumes become straight-sided.

https://doi.org/10.1017/jfm.2014.246 Published online by Cambridge University Press

Axisymmetric straight-sided plume solutions in stratified environments have recently received attention in Kaye & Scase (2011).

Extending the approach of van den Bremer & Hunt (2010) for axisymmetric plumes to planar plumes, we show that provided we introduce 'universal notation' and adopt a suitable scaling, the solutions to the systems of equations describing Boussinesq and non-Boussinesq plumes take the same mathematical form, which in turn highlights the analogies and differences between the two in a powerful and effective way. In doing so, a length scale is identified on which the transition between Boussinesq and non-Boussinesq behaviour takes place. This length scale is of a similar form but altogether different to the transition length scale for axisymmetric plumes rising from point sources derived by Rooney (1997) and generalized to area sources by van den Bremer & Hunt (2010). The implications of the unmodified entrainment assumption underlying this universality for the prediction of the physical behaviour of a non-Boussinesq plume, compared to the prediction of the behaviour of such a plume by a Boussinesq model, raise significant questions regarding the validity of this assumption. This is explored in detail in the accompanying paper (van den Bremer & Hunt 2014).

This paper is laid out as follows: § 2 introduces the plume conservation equations and these are rewritten in a non-dimensional form that is potentially universally applicable to Boussinesq and non-Boussinesq plumes and Boussinesq fountains. The different entrainment models with constant α for Boussinesq and non-Boussinesq plumes and Boussinesq fountains, and with varying $\alpha = \alpha(\Gamma)$ for forced Boussinesq plumes are also discussed in § 2. The universal solutions for pure jets ($\Gamma_0 = 0$), pure plumes ($\Gamma_0 = 1$), fountains ($\Gamma_0 < 0$), forced plumes ($0 < \Gamma_0 < 1$) and lazy plumes ($\Gamma_0 > 1$) all with constant α, and the solutions for forced plumes ($0 < \Gamma_0 < 1$) with variable α are presented in § 3. The characteristic behaviour of fountains and of forced and lazy plumes is examined in § 4, and the discussion is aided by the presentation of scale diagrams. Far-field behaviour and the transition between non-Boussinesq and Boussinesq behaviour is discussed in § 5. Finally, conclusions are drawn in § 6.

2. Plume model

2.1. *Similarity*

In order to describe the bulk time-averaged behaviour of turbulent plumes and fountains with height it is necessary to model the horizontal variation across the plume width. By averaging along the axis of symmetry of the plume, variations along the length of the plume are ignored; the cross-section-integrated quantities used hereinafter are therefore per-unit-length without exception. The most commonly adopted profiles to describe the time-averaged horizontal variation of vertical velocity and density across the plume width are Gaussian and top-hat profiles. For planar Boussinesq plumes, Gaussian profiles are given by the vertical velocity $w(x, z) = w_m(z)\exp(-x^2/b^2)$ and reduced gravity $g'(x, z) = g'_m(z)\exp(-x^2/b^2)$, where x is the (cross-stream) horizontal coordinate orthogonal to the vertical axis of symmetry, z is the vertical coordinate measured from the source upwards, w_m and g'_m are the centreline values of the vertical velocity and the reduced gravity, respectively, and b is a characteristic measure of the plume half-width. The characteristic measure of the plume half-width based on the velocity and the reduced density profiles may be different. The reduced gravity $g' = g(\rho_a - \rho)/\rho_a = g(1 - \eta)$ and the density contrast is defined as:

$$\eta(x, z) \equiv \frac{\rho(x, z)}{\rho_a}, \tag{2.1}$$

https://doi.org/10.1017/jfm.2014.246 Published online by Cambridge University Press

where $\rho(x, z)$ is the local density of the plume fluid after averaging in time and along the axis of the plume and ρ_a the (constant) density of the ambient fluid. For non-Boussinesq plumes, measurements of the precise form of these cross-stream profiles are rare and not conclusive. The debate in the literature has therefore revolved around the question of which quantity should be described by a Gaussian distribution based on theoretical arguments, $1-\eta=(\rho_a-\rho)/\rho_a$ or $(1-\eta)/\eta=(\rho_a-\rho)/\rho$, and what the most appropriate length scale is on which the horizontal coordinate x in the exponent should be scaled, where the scale for the velocity and the effective gravity profiles may be different. In the absence of experimental data, similarity arguments cannot unequivocally answer these questions. By defining a true similarity solution as one for which the mass flux near the origin can be set to zero, Thomas & Delichatsios (2007) attempt to resolve this debate. However, their length scale on which the horizontal coordinate x must be scaled is only defined through an implicit function of the local vertical velocity and the local density contrast, resulting in solutions that are perhaps overly complex.

Although it is evident that Gaussian profiles generally provide a better fit to cross-sectional data, top-hat profiles are adopted herein as they considerably simplify the analysis and thus lend greater insight into the bulk behaviour of the release with height. The difference between the conservation equations for top-hat and Gaussian profiles is one of coefficients; the form of the conservation equations and the nature of the predicted behaviour are equivalent. Indeed, it can be shown (appendix A for the Boussinesq case and appendix B, where the argument of Thomas & Delichatsios 2007 is reproduced, for the non-Boussinesq case) that the solutions presented in this article are valid for Boussinesq plumes with top-hat profiles and Gaussian profiles alike. It should be emphasized that, in the absence of careful measurements for non-Boussinesq plumes, the choice of which variable, $(1-\eta)$ or $(1-\eta)/\eta$, is best described by a Gaussian distribution remains an arbitrary one.

2.2. *Conservation equations*

Adopting top-hat profiles, for an unstratified quiescent ambient, the equations expressing conservation of mass and momentum prior to applying the Boussinesq approximation can be respectively written as follows:

$$\frac{\mathrm{d}(2\eta wb)}{\mathrm{d}z}=2u_e, \tag{2.2}$$

$$\frac{\mathrm{d}(2\eta w^2 b)}{\mathrm{d}z}=2b(1-\eta)g, \tag{2.3}$$

where u_e is the horizontal entrainment velocity at the edge ($x=\pm b$) of the top-hat profile of the plume. For top-hat profiles the fluxes of mass G and momentum M, normalized by the ambient density ρ_a, and the volume flux Q are:

$$G=2\eta wb, \quad M=2\eta w^2 b, \quad Q=2wb. \tag{2.4a–c}$$

As is standard, it has been assumed in deriving the equation for conservation of momentum (2.3) that the plume is long and thin so that vertical pressure gradients are much greater than cross-stream pressure gradients.

The Boussinesq approximation, which can be made if the density contrast between the ambient and release fluids is suitably small, is two-fold. The variation in density

https://doi.org/10.1017/jfm.2014.246 Published online by Cambridge University Press

on the left-hand side of (2.2) can be ignored, so that $G = 2\eta wb$ can be replaced by $Q = 2wb$; conservation of mass flux implies conservation of volume flux under the Boussinesq approximation. Secondly, $M = 2\eta w^2 b$ can be replaced by $M_B = 2w^2 b$ on the left-hand side of (2.3), ignoring the contribution of density variation to changes in the momentum flux.

In the non-Boussinesq case, assuming the plume fluid behaves as an ideal gas, there is no external heat input into the plume, the pressure variation in the ambient is hydrostatic, and restricting our attention to length scales much smaller than the length scale associated with the hydrostatic pressure distribution of the ambient ($L_H = p_a/g\rho_a$, where p_a is the ambient pressure), it can also be shown that volume is conserved. The derivation originally made by Rooney & Linden (1996) is reproduced in the review by van den Bremer & Hunt (2010) in its simplest form for the axisymmetric case. In both the Boussinesq and the non-Boussinesq cases, conservation of volume flux takes the form:

$$\frac{\mathrm{d}(2wb)}{\mathrm{d}z} = 2u_e. \tag{2.5}$$

Combining conservation of volume flux (2.5) and conservation of mass flux (2.2) yields conservation of the flux of density deficit, i.e. conservation of the quantity:

$$B = 2g(1-\eta)wb, \tag{2.6}$$

which has the dimensions of buoyancy flux L^3T^{-3} and becomes equal to the buoyancy flux in the Boussinesq limit. This quantity is conserved for both the Boussinesq and the non-Boussinesq cases.

The conservation equations ((2.2), (2.3) and (2.5)) are also valid for planar fountains (Hunt & Coffey 2009), governing the behaviour until the initial maximum rise height is reached but not the subsequent collapse, where the dynamics of entrainment are significantly modified and momentum is exchanged between upflowing and downflowing bodies of fluid.

2.3. *The entrainment model*

To achieve turbulence closure, it is necessary to model the entrainment of the ambient fluid. Herein, we adopt the entrainment model originally adopted by Lee & Emmons (1961) based on the seminal entrainment model of Taylor (1945) and popularized by Morton *et al.* (1956):

$$u_e = \alpha w \quad \text{for Boussinesq and non-Boussinesq plumes,} \tag{2.7}$$

where α is a constant. This entrainment model is consistent with the simplest class of (similarity) solution to the system of ordinary differential equations ((2.2), (2.3) and (2.5)), namely the solution for plumes rising from line sources (cf. the point-source solutions for axisymmetric plumes by Morton *et al.* 1956), in which the fluxes of mass and momentum can be expressed as powers of height z, and which can be derived based on dimensional arguments. These line-source solutions are given in appendix C in terms of the universal notation introduced in § 2.4.

Throughout our primary theoretical developments, we adopt entrainment coefficients that are pertinent for top-hat profiles, denoting this coefficient as α. As such, rather than introduce subscripts to distinguish between top-hat and Gaussian values, we note that the only exceptions are (i) the entries in table 1 (where we list Gaussian entrainment coefficients resulting from experimental studies) and (ii) in (2.15) and

https://doi.org/10.1017/jfm.2014.246 Published online by Cambridge University Press

	Spreading rate (db/dz)	α	Release type
Kotsovinos (1975) literature review (table 1.3.1)	—	0.04–0.06	Pure jet
Kotsovinos (1976)	0.14	0.06	Pure jet
Chen & Rodi (1980)	0.11–0.14	0.05–0.06	Pure jet
Antonia *et al.* (1983)	0.10	0.05	Pure jet
Lee & Emmons (1961)	—	0.16	Pure plume
Kotsovinos (1975)	—	0.10	Pure plume
Chen & Rodi (1980) (Rouse *et al.* (1952) revised)	0.12–0.13	0.11–0.12	Pure plume
Yuan & Cox (1996)	—	0.13	Pure plume

TABLE 1. Overview of experimentally determined values of the (constant) slope of the plume envelope db/dz or 'spreading rate' and the entrainment coefficient that is derived from this constant spreading rate in the majority of cases. As observations generally support Gaussian cross-stream profiles, we then have for pure jets $db/dz = 4\alpha/\sqrt{\pi}$ and for pure plumes $db/dz = 2\alpha/\sqrt{\pi}$ (appendix A), where α is the (Gaussian) entrainment coefficient. Where multiple values are quoted, this reflects the use of different half-width scales used to characterize the variation of the (approximately normally distributed) buoyancy and vertical velocity profiles. In the case of Kotsovinos (1975) literature review, the range reflects the different other authors cited in that work (see table 1.3.1 of Kotsovinos 1975).

appendices A and B where the entrainment coefficient is Gaussian in order to highlight how our results can be applied to a Gaussian plume model.

Contrary to the axisymmetric case (van den Bremer & Hunt 2010), the horizontal entrainment velocity suggested by similarity arguments (2.7) is unaffected by non-Boussinesq effects. As recognized by Delichatsios (1988), there is no experimental evidence to either support or contradict this result. It is, thus, only founded on consistency with similarity solutions, namely the line-source solutions given in appendix C. For further discussion, see Rooney (1997). In the axisymmetric case there is experimental evidence, albeit limited, to support a modified entrainment model that predicts a reduction of the entrainment velocity for increasing density contrasts. The independence of the entrainment model from the density contrast in the planar case is in contradiction with the axisymmetric case, for which self-similarity implies a reduction of the entrainment velocity by a factor $\sqrt{\eta}$ (cf. $u_e = \alpha w\sqrt{\eta}$). The tentative hypothesis of Delichatsios (1988) that the entrainment velocity is unaffected by non-Boussinesq effects can readily be adopted, resulting in the universal solutions discussed in § 2.4.

As an alternative to the constant entrainment coefficient model in (2.7), entrainment models have been proposed in which the entrainment coefficient varies linearly with the local flux balance. This reflects the observation that the entrainment coefficient is generally larger for buoyant jets than for pure jets, a phenomenon that can be explained by buoyancy-enhanced turbulence. Although this assumption is not made explicitly, Kotsovinos & List (1977) assume that α varies linearly with the local value of Γ and find that it gives a better description for forced plumes. For forced plumes, we examine the effects on the model outcome of the following entrainment model:

$$u_e = (\alpha_j + (\alpha_p - \alpha_j)\Gamma)w = \alpha_p(\kappa + (1-\kappa)\Gamma)w \quad \text{for } 0 \leqslant \Gamma \leqslant 1, \tag{2.8}$$

https://doi.org/10.1017/jfm.2014.246 Published online by Cambridge University Press

where α_j is the entrainment coefficient for a pure jet, α_p the entrainment coefficient for a pure plume and $\kappa = \alpha_j/\alpha_p$. For $\kappa = 1$ we recover the constant-coefficient entrainment model in (2.7).

Although experimental measurements of the entrainment coefficient α vary (see table 1 for an overview of values of the entrainment coefficient for Gaussian profiles found in the literature, where we emphasize that many authors have adopted different definitions of the entrainment coefficient and great care in comparing experimentally obtained values is imperative), the evidence seems supportive of the entrainment coefficient for pure plumes being at least two times larger than the entrainment coefficient for pure jets. As shown in § 3.5, forced plumes become straight-sided for $\kappa = 1/2$. List & Imberger (1973) provide an alternative rationale for the entrainment model in (2.8) with $\kappa = 1/2$ from observations that a forced plume is indeed straight-sided. List & Imberger (1973) thereby provided evidence for the earlier hypothesis of Priestley & Ball (1955), who did not make an explicit entrainment assumption, but instead assumed a particular form of the Reynolds stress distribution. For axisymmetric fountains there is evidence that the entrainment coefficient is significantly reduced by negative buoyancy (Kaminski, Tait & Carazzo 2005), but such variation is not considered further herein for planar fountains.

2.4. *Universal solutions*

Having adopted the standard entrainment model (2.7), the conservation equations for the fluxes of mass, volume and momentum are equivalent to those of Lee & Emmons (1961) for Boussinesq plumes. The analogy with the conservation equations of Morton *et al.* (1956) cannot be missed. Also adopting the entrainment model (2.7) for non-Boussinesq plumes, the conservation equations can be written in a universal form:

$$\frac{\mathrm{d}\mathscr{G}}{\mathrm{d}z} = 2u_e, \qquad \frac{\mathrm{d}\mathscr{M}}{\mathrm{d}z} = \frac{B\mathscr{G}}{\mathscr{M}}, \qquad \frac{\mathrm{d}B}{\mathrm{d}z} = 0, \tag{2.9a–c}$$

where we use the following notation:

$$\mathscr{G} = \begin{cases} 2wb = Q, \\ 2\eta wb = G, \end{cases} \qquad \mathscr{M} = \begin{cases} 2w^2 b = M_B & \text{(Boussinesq)}, \\ 2\eta w^2 b = M & \text{(non-Boussinesq)}. \end{cases} \tag{2.10a,b}$$

Accordingly, we define the effective half-width β and the density parameter Δ:

$$\beta = \begin{cases} b, \\ b\eta, \end{cases} \qquad \Delta = \begin{cases} 1-\eta & \text{(Boussinesq)}, \\ \dfrac{1-\eta}{\eta} & \text{(non-Boussinesq)}, \end{cases} \tag{2.11a,b}$$

so that $\mathscr{G} = 2w\beta$ and $\mathscr{M} = 2w^2\beta$.

2.5. *Γ-approach for constant α*

Adopting the universal notation in (2.10) and (2.11), the flux balance parameter Γ for a constant entrainment coefficient α can be defined as:

$$\Gamma = \frac{B\mathscr{G}^3}{2\alpha\mathscr{M}^3} = \frac{g\beta\Delta}{\alpha w^2} = \frac{gb(1-\eta)}{\alpha w^2}, \tag{2.12}$$

https://doi.org/10.1017/jfm.2014.246 Published online by Cambridge University Press

so that the line-source solutions in appendix C correspond to $\Gamma = 1$, i.e. a plume that is pure at all heights. Furthermore, it can be noted both from the ratio of $\mathscr{G}$ and $\mathscr{M}$ on the left-hand side of (2.12) and from the far right-hand-side term, that Γ takes the same value if a given plume is modelled by either a Boussinesq or a non-Boussinesq model.

After considerable manipulation the equations of conservation of the fluxes of volume, momentum and buoyancy (2.9) can be expressed in terms of Γ, the non-dimensional effective half-width $\hat{\beta} = \beta/\beta_0$, the non-dimensional velocity $\hat{w} = w/w_0$ and a non-dimensional height $\zeta = \alpha z/\beta_0$:

$$\frac{\mathrm{d}\Gamma}{\mathrm{d}\zeta} = \frac{3\Gamma(1-\Gamma)}{\hat{\beta}}, \quad \frac{\mathrm{d}\hat{\beta}}{\mathrm{d}\zeta} = 2 - \Gamma, \quad \frac{\mathrm{d}\hat{w}}{\mathrm{d}\zeta} = \frac{\hat{w}}{\hat{\beta}}(\Gamma - 1). \tag{2.13a–c}$$

Note that the definition of the non-dimensional height ζ depends on β_0 and, therefore, is different in Boussinesq and non-Boussinesq cases.

The system of ordinary differential equations (2.13) can be solved subject to the initial conditions:

$$\Gamma = \Gamma_0, \quad \hat{\beta} = 1, \quad \hat{w} = 1 \quad \text{at} \quad \zeta = 0. \tag{2.14a–c}$$

As for the axisymmetric case (van den Bremer & Hunt 2010), there are five classes of solution: fountains ($\Gamma_0 < 0$), pure jets ($\Gamma_0 = 0$), forced plumes ($0 < \Gamma_0 < 1$), pure plumes ($\Gamma_0 = 1$) and lazy plumes ($\Gamma_0 > 1$).

Equations (2.13) and hence the solutions presented hereinafter are equally valid for Boussinesq (appendix A) and non-Boussinesq plumes (appendix B following Thomas & Delichatsios 2007 with $\lambda = 1$) with Gaussian profiles and in that case:

$$\Gamma = \frac{B\mathscr{G}^3}{2^{3/2}\alpha\mathscr{M}^3}, \quad \zeta = \frac{2\alpha}{\sqrt{\pi}}\frac{z}{\beta_0} \quad \text{(Gaussian profiles)}, \tag{2.15a,b}$$

with α now denoting the value of the entrainment coefficient for Gaussian profiles.

2.6. Γ-approach for variable α

Adopting an entrainment coefficient $\alpha(\Gamma)$ that varies linearly with the local Richardson number (2.8), the entrainment coefficient in the definition of Γ (2.12) is replaced by the (constant) entrainment coefficient for pure plumes α_p:

$$\Gamma = \frac{BQ^3}{2\alpha_p M_B^3} = \frac{gb(1-\eta)}{\alpha_p w^2}. \tag{2.16}$$

The entrainment model with a variable entrainment coefficient is only examined for the Boussinesq case. Furthermore, it is only valid for the range $0 < \Gamma_0 < 1$, as it is pertinent only for forced releases. Universal notation is therefore not adopted in this section. With the entrainment model (2.8) and the modified definition of Γ (2.16), the conservation equations can be expressed in terms of $\hat{w} = w/w_0$, $\hat{b} = b/b_0$, Γ and $\zeta = \alpha_p z/b_0$:

$$\frac{\mathrm{d}\Gamma}{\mathrm{d}\zeta} = \frac{3\kappa\Gamma(1-\Gamma)}{\hat{b}}, \quad \frac{\mathrm{d}\hat{b}}{\mathrm{d}\zeta} = 2\kappa - (2\kappa - 1)\Gamma, \quad \frac{\mathrm{d}\hat{w}}{\mathrm{d}\zeta} = \frac{\hat{w}}{\hat{b}}\kappa(\Gamma - 1). \tag{2.17a–c}$$

In the specific case $\kappa = 1/2$, which is in close agreement with experimentally (§ 2.3) inferred values of the entrainment coefficient, a new class of solution arises for which (forced) plumes become straight-sided (§ 3.5) in addition to the solutions given in §§ 3.1–3.3.

https://doi.org/10.1017/jfm.2014.246 Published online by Cambridge University Press

3. Solutions to the plume equations

3.1. *Pure jets ($\eta_0 = 1,\ \Gamma_0 = 0$)*

For releases arising from finite non-zero width sources, $\Gamma_0 = 0$ must correspond to $\eta_0 = \eta(z) = 1$, i.e. a pure jet with zero buoyancy flux. For a pure jet, (2.12) requires that $\Gamma(z) = \Gamma_0 = 0$. Equations (2.13) have the following solutions for b and w:

$$\frac{b}{b_0} = 1 + 2\zeta, \quad \frac{w}{w_0} = \frac{1}{\sqrt{1+2\zeta}}. \tag{3.1a,b}$$

The solutions (3.1) can be combined to give the solutions for the fluxes of volume and momentum:

$$\frac{Q}{Q_0} = \sqrt{1+2\zeta}, \quad \frac{M_B}{M_{B,0}} = 1. \tag{3.2a,b}$$

3.2. *Pure plumes ($\eta_0 < 1,\ \Gamma_0 = 1$)*

For pure plumes ($\eta_0 < 1$) from finite non-zero width sources, (2.13) requires $\Gamma(z) = \Gamma_0 = 1$. Equations (2.13), combined with the definition of Γ (2.12), have solutions for β, w and Δ:

$$\frac{\beta}{\beta_0} = 1 + \zeta, \quad \frac{w}{w_0} = 1, \quad \frac{\Delta}{\Delta_0} = \frac{1}{1+\zeta}. \tag{3.3a–c}$$

The solutions (3.3) can be combined to give the fluxes:

$$\frac{\mathscr{G}}{\mathscr{G}_0} = 1 + \zeta, \quad \frac{\mathscr{M}}{\mathscr{M}_0} = 1 + \zeta. \tag{3.4a,b}$$

We note that the solutions (3.3) and (3.4) for pure plumes from non-zero width sources are equivalent to those for pure plumes rising from line sources (appendix C) in terms of their behaviour with respect to height with an origin correction $\zeta_{oc} = -1$. This pure plume solution is exact at all heights, noting a singularity at the origin $\zeta = \zeta_{oc} = -1$ for the density parameter Δ in (3.3*c*).

3.3. *Fountains ($\eta_0 > 1,\ \Gamma_0 < 0$), forced plumes ($\eta_0 < 1,\ 0 < \Gamma_0 < 1$) and lazy plumes ($\eta_0 < 1,\ \Gamma_0 > 1$) with constant α*

Solving the conservation equations for Γ and $\hat{\beta}$ in (2.13) simultaneously gives the scaled effective half-width $\hat{\beta}$ as a function of Γ and Γ_0 for fountains ($\eta_0 > 1,\ \Gamma_0 < 0$), forced plumes ($\eta_0 < 1,\ 0 < \Gamma_0 < 1$) and lazy plumes ($\eta_0 < 1,\ \Gamma_0 > 1$):

$$\frac{\beta}{\beta_0} = \left(\frac{\Gamma}{\Gamma_0}\right)^{2/3} \left(\frac{1-\Gamma_0}{1-\Gamma}\right)^{1/3}. \tag{3.5}$$

Substituting (3.5) back into the expression for $\mathrm{d}\Gamma/\mathrm{d}\zeta$ from (2.13) gives the vertical rate of change of the flux balance parameter Γ:

$$\frac{\mathrm{d}\Gamma}{\mathrm{d}\zeta} = 3\Gamma(1-\Gamma)\left(\frac{\Gamma_0}{\Gamma}\right)^{2/3} \left(\frac{1-\Gamma}{1-\Gamma_0}\right)^{1/3}. \tag{3.6}$$

https://doi.org/10.1017/jfm.2014.246 Published online by Cambridge University Press

Integrating (3.6) gives the height ζ at which a certain value of Γ is attained for the three classes of solution:

$$\zeta = \begin{cases} -\dfrac{1}{3}\dfrac{(1-\Gamma_0)^{1/3}}{(-\Gamma_0)^{2/3}}\displaystyle\int_{\Gamma_0}^{\Gamma}\frac{\mathrm{d}x}{(-x)^{1/3}(1-x)^{4/3}} & \text{for } \Gamma_0 < 0, \\ \dfrac{1}{3}\dfrac{(1-\Gamma_0)^{1/3}}{\Gamma_0^{2/3}}\displaystyle\int_{\Gamma_0}^{\Gamma}\frac{\mathrm{d}x}{x^{1/3}(1-x)^{4/3}} & \text{for } 0 < \Gamma_0 < 1, \\ -\dfrac{1}{3}\dfrac{(\Gamma_0-1)^{1/3}}{\Gamma_0^{2/3}}\displaystyle\int_{\Gamma_0}^{\Gamma}\frac{\mathrm{d}x}{x^{1/3}(x-1)^{4/3}} & \text{for } \Gamma_0 > 1, \end{cases} \tag{3.7}$$

where x is a dummy variable. Although (3.7) has a closed-form solution in the form of a hypergeometric series, we do not detail this solution here as the series solution does not lend more insight than numerical evaluation of the integral and far-field asymptotics discussed in § 5.1. Combining the conservation equations for $\hat{w}$ and Γ in (2.13) yields the vertical velocity as a function of Γ and Γ_0:

$$\frac{w}{w_0} = \left(\frac{\Gamma_0}{\Gamma}\right)^{1/3}. \tag{3.8}$$

The rate of change of vertical velocity with height can then be found by substituting (3.5) and (3.8) into the expression for $\mathrm{d}\hat{w}/\mathrm{d}\zeta$ in (2.13):

$$\frac{\mathrm{d}\hat{w}}{\mathrm{d}\zeta} = -(1-\Gamma)\frac{\Gamma_0}{\Gamma}\left(\frac{1-\Gamma}{1-\Gamma_0}\right)^{1/3}. \tag{3.9}$$

The rate of change of the effective half-width with height (the slope of the plume envelope) is simply given by:

$$\frac{\mathrm{d}\hat{\beta}}{\mathrm{d}\zeta} = 2 - \Gamma. \tag{3.10}$$

Combining the solutions for $\hat{\beta}$ (3.5), $\hat{w}$ (3.8) and the definition of Γ (2.12), the dimensionless density parameter $\hat{\Delta} = \Delta/\Delta_0$ and fluxes $\hat{\mathscr{G}} = \mathscr{G}/\mathscr{G}_0$ and $\hat{\mathscr{M}} = \mathscr{M}/\mathscr{M}_0$ can be expressed as:

$$\frac{\Delta}{\Delta_0} = \left(\frac{\Gamma_0}{\Gamma}\right)^{1/3}\left(\frac{1-\Gamma}{1-\Gamma_0}\right)^{1/3}, \quad \frac{\mathscr{G}}{\mathscr{G}_0} = \left(\frac{\Gamma}{\Gamma_0}\right)^{1/3}\left(\frac{1-\Gamma_0}{1-\Gamma}\right)^{1/3}, \quad \frac{\mathscr{M}}{\mathscr{M}_0} = \left(\frac{1-\Gamma_0}{1-\Gamma}\right)^{1/3}. \tag{3.11a–c}$$

In general throughout this paper, hatted variables refer to those variables scaled on their source values. The rate of change of $\hat{\Delta}$, $\hat{\mathscr{G}}$ and $\hat{\mathscr{M}}$ with height can be found by combining the derivatives with respect to Γ of each term in (3.11), respectively, with $\mathrm{d}\Gamma/\mathrm{d}\zeta$ from (3.6):

$$\frac{\mathrm{d}\hat{\Delta}}{\mathrm{d}\zeta} = -\frac{\Gamma_0}{\Gamma}\left(\frac{1-\Gamma}{1-\Gamma_0}\right)^{2/3}, \quad \frac{\mathrm{d}\hat{\mathscr{G}}}{\mathrm{d}\zeta} = \left(\frac{\Gamma_0}{\Gamma}\right)^{1/3}, \quad \frac{\mathrm{d}\hat{\mathscr{M}}}{\mathrm{d}\zeta} = \Gamma\left(\frac{\Gamma_0}{\Gamma}\right)^{2/3}. \tag{3.12a–c}$$

https://doi.org/10.1017/jfm.2014.246 Published online by Cambridge University Press

3.4. *Forced plumes with variable α*

For (Boussinesq) forced plumes with an entrainment coefficient α that varies linearly with Γ (2.8), the conservation equations for $\hat{b}$ and Γ in (2.17) combine to give:

$$\frac{b}{b_0} = \left(\frac{\Gamma}{\Gamma_0}\right)^{2/3} \left(\frac{1-\Gamma_0}{1-\Gamma}\right)^{1/(3\kappa)}, \tag{3.13}$$

which reduces to (3.5) for $\kappa = 1$. Substituting for $\hat{b}$ from (3.13) into $\mathrm{d}\Gamma/\mathrm{d}\zeta$ in (2.17) gives:

$$\frac{\mathrm{d}\Gamma}{\mathrm{d}\zeta} = 3\kappa\Gamma(1-\Gamma)\left(\frac{\Gamma_0}{\Gamma}\right)^{2/3} \left(\frac{1-\Gamma}{1-\Gamma_0}\right)^{1/(3\kappa)}, \tag{3.14}$$

which can be readily integrated from the source to a given height ζ:

$$\zeta = \frac{1}{3\kappa} \frac{(1-\Gamma_0)^{1/(3\kappa)}}{\Gamma_0^{2/3}} \int_{\Gamma_0}^{\Gamma} \frac{\mathrm{d}x}{x^{1/3}(1-x)^{1+(1/(3\kappa))}}. \tag{3.15}$$

The solution for $\hat{w}$ can be found by combining the conservation equations for $\hat{w}$ and Γ (2.17), and solving the resulting ordinary differential equation:

$$\frac{w}{w_0} = \left(\frac{\Gamma_0}{\Gamma}\right)^{1/3}. \tag{3.16}$$

We note that the solution for the vertical velocity (3.16) is independent of the entrainment coefficient ratio κ. As for plumes with a constant entrainment coefficient, combining the solutions for $\hat{b}$ (3.13) and $\hat{w}$ (3.16) and the definition of Γ (2.16), the scaled density parameter $\hat{\Delta}$ and the scaled fluxes of volume $\hat{Q}$ and momentum $\hat{M}_B$ can be expressed as:

$$\frac{\Delta}{\Delta_0} = \left(\frac{\Gamma_0}{\Gamma}\right)^{1/3} \left(\frac{1-\Gamma}{1-\Gamma_0}\right)^{1/(3\kappa)}, \quad \frac{Q}{Q_0} = \left(\frac{\Gamma}{\Gamma_0}\right)^{1/3} \left(\frac{1-\Gamma_0}{1-\Gamma}\right)^{1/(3\kappa)}, \quad \frac{M_B}{M_{B,0}} = \left(\frac{1-\Gamma_0}{1-\Gamma}\right)^{1/(3\kappa)}. \tag{3.17a–c}$$

The rate of change of $\hat{\Delta}$, $\hat{Q}$ and $\hat{M}_B$ with height can be found by combining the derivatives with respect to Γ of each term in (3.17), respectively, with $\mathrm{d}\Gamma/\mathrm{d}\zeta$ from (3.14):

$$\frac{\mathrm{d}\hat{\Delta}}{\mathrm{d}\zeta} = -\frac{\Gamma_0}{\Gamma}\left(\frac{1-\Gamma}{1-\Gamma_0}\right)^{2/(3\kappa)} \big(\kappa(1-\Gamma)+\Gamma\big), \quad \frac{\mathrm{d}\hat{Q}}{\mathrm{d}\zeta} = \left(\frac{\Gamma_0}{\Gamma}\right)^{1/3} \big(\kappa(1-\Gamma)+\Gamma\big), \tag{3.18a,b}$$

$$\frac{\mathrm{d}\hat{M}_B}{\mathrm{d}\zeta} = \Gamma\left(\frac{\Gamma_0}{\Gamma}\right)^{2/3}. \tag{3.18c}$$

3.5. *Straight-sided forced plumes*

It is evident from (2.17*b*) that for $\kappa = \alpha_j/\alpha_p = 1/2$, planar forced plumes become straight-sided. The slope of the plume envelope is equal to that of a pure plume

https://doi.org/10.1017/jfm.2014.246 Published online by Cambridge University Press

(3.3) ($\mathrm{d}\hat{b}/\mathrm{d}\zeta = 1$ in both cases), and exact solutions can be found to the system of conservation equations (2.17):

$$\frac{b}{b_0} = 1 + \zeta, \quad \Gamma = \frac{1}{1 + \dfrac{1-\Gamma_0}{\Gamma_0}(1+\zeta)^{-3/2}}, \quad \frac{w}{w_0} = (\Gamma_0 + (1-\Gamma_0)(1+\zeta)^{-3/2})^{1/3}. \tag{3.19a,b,c}$$

The solutions (3.19) can be combined with the definition of Γ (2.16) to give:

$$\frac{\Delta}{\Delta_0} = \frac{1}{\Gamma_0^{1/3}}\left((1+\zeta)^3 + \frac{1-\Gamma_0}{\Gamma_0}(1+\zeta)^{3/2}\right)^{-1/3}, \tag{3.20a}$$

$$\frac{Q}{Q_0} = (\Gamma_0(1+\zeta)^3 + (1-\Gamma_0)(1+\zeta)^{3/2})^{1/3}, \tag{3.20b}$$

$$\frac{M_B}{M_{B,0}} = (\Gamma_0(1+\zeta)^{3/2} + 1 - \Gamma_0)^{2/3}. \tag{3.20c}$$

4. Characteristic behaviour

As for the axisymmetric case (cf. Morton & Middleton 1973), the unique features of planar plumes and fountains and their variation with the source conditions can be illustrated by plotting certain scaled characteristic heights as a function of the source parameter Γ_0 (figures 1 and 2). The characteristic behaviour of the three main types of release, fountains (§ 4.1), forced plumes (§ 4.2) and lazy plumes (§ 4.3), is discussed below. In each section, the results are illustrated by a series of figures (figures 3–6) that show the outline of the plume or fountain envelope $\hat{b}$ as it varies with height for different values of Γ_0. Another series of graphs (figures 7–11) explores the variation of the quantities Γ, $\hat{\Delta}$, $\hat{w}$, $\hat{\mathscr{G}}$ and $\hat{\mathscr{M}}$ with height by plotting contours of constant values of these quantities and their derivatives with respect to height in (Γ_0, ζ)-space. In addition, table 2 shows the values of the derivatives at the source ($\zeta = 0$) (for plumes and fountains) and asymptotically far away from the source ($\zeta \to \infty$) (for plumes).

4.1. *Fountains*

For Boussinesq fountains with a constant entrainment coefficient, the only type of fountain considered herein, the characteristic heights shown in figure 1 are the initial rise height (ζ_{irh}) and the height at which the magnitude of the acceleration ($|\hat{w}'| = |\mathrm{d}\hat{w}/\mathrm{d}\zeta|$) reaches a minimum ($\zeta_{|\hat{w}'|_{min}}$). It can be readily observed from figure 3 that fountains, unless highly forced, become relatively broad (large $\mathrm{d}b/\mathrm{d}z$) compared to forced and lazy plumes (cf. figures 4 and 5) resulting in pressure gradients in the horizontal direction no longer being much smaller than those in the vertical, which is likely to invalidate the 'long and thin' assumption made in deriving the conservation equations. As the momentum flux is eroded, from that imparted to the fountain from its source, by the momentum flux induced by the opposing buoyancy flux, a fountain will reach a maximum rise height corresponding to $b \to \infty$ and $w \to 0$ and, therefore to $\Gamma \to -\infty$. This rise height $\zeta = \zeta_{irh}$ is termed the initial rise height after Turner (1966) and is given by taking the limit $\Gamma = -\infty$ of (3.7):

$$\zeta_{irh} = -\frac{1}{3}\frac{(1-\Gamma_0)^{1/3}}{(-\Gamma_0)^{2/3}}\int_{\Gamma_0}^{-\infty}\frac{\mathrm{d}x}{(-x)^{1/3}(1-x)^{4/3}}. \tag{4.1}$$

https://doi.org/10.1017/jfm.2014.246 Published online by Cambridge University Press

	Γ	$\frac{\mathrm{d}\Gamma}{\mathrm{d}\zeta}$	$\frac{\mathrm{d}\hat{w}}{\mathrm{d}\zeta}$	$\frac{\mathrm{d}\hat{\beta}}{\mathrm{d}\zeta}$	$\frac{\mathrm{d}\hat{\Delta}}{\mathrm{d}\zeta}$	$\frac{\mathrm{d}\hat{\mathscr{G}}}{\mathrm{d}\zeta}$	$\frac{\mathrm{d}\hat{\mathscr{M}}}{\mathrm{d}\zeta}$
$\kappa=1$: $\zeta=0$	Γ_0	$3\Gamma_0(1-\Gamma_0)$	Γ_0-1	$2-\Gamma_0$	-1	1	Γ_0
$\kappa=1/2$: $\zeta=0$	Γ_0	$\frac{3\Gamma_0(1-\Gamma_0)}{2}$	$\frac{\Gamma_0-1}{2}$	1	$-\frac{1+\Gamma_0}{2}$	$\frac{1+\Gamma_0}{2}$	Γ_0
$\kappa=1$: $\zeta\to\infty$	1	0	0	1	0	$\Gamma_0^{1/3}$	$\Gamma_0^{2/3}$
$\kappa=1/2$: $\zeta\to\infty$	1	0	0	1	0	$\Gamma_0^{1/3}$	$\Gamma_0^{2/3}$

TABLE 2. Values of the derivatives of plume quantities and fluxes at the sources ($\zeta=0$) and in the limit $\zeta\to\infty$ ($\Gamma=1$) for a constant entrainment coefficient ($\kappa=1$) and a variable entrainment coefficient $\kappa=1/2$. The first row ($\kappa=1:\zeta=0$) is valid for Boussinesq fountains ($\Gamma_0<0$) and both non-Boussinesq and Boussinesq forced and lazy plumes ($\Gamma_0>0$), whereas the second row ($\kappa=1/2:\zeta=0$) is only valid for forced Boussinesq plumes ($0<\Gamma_0<1$). The third row ($\kappa=1:\zeta\to\infty$) is valid for both non-Boussinesq and Boussinesq forced and lazy plumes ($\Gamma_0>0$), whereas the fourth row ($\kappa=1/2:\zeta\to\infty$) is only valid for forced Boussinesq plumes ($0<\Gamma_0<1$).

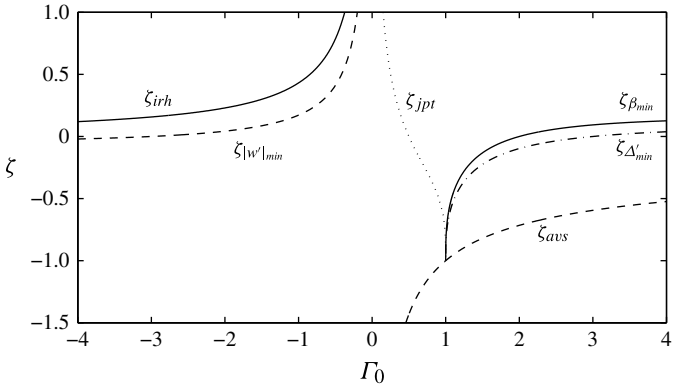

FIGURE 1. Scale diagram for planar fountains, forced plumes and lazy plumes showing the initial rise height ζ_{irh}, the minimum deceleration height $\zeta_{|w'|_{min}}$, the jet–plume transition height ζ_{jpt}, the minimum effective half-width neck height $\zeta_{\beta_{min}}$, the maximum dilution rate height $\zeta_{\Delta'_{min}}$ and the asymptotic virtual source correction ζ_{avs}.

Table 3 shows the values that the different quantities attain at the initial rise height. Solutions for fountains are based on the plume entrainment model, which becomes invalid after the fountain has reached its initial rise height and reverses because of subsequent interaction between upflow and downflow. Hunt & Coffey (2009) further subdivided the fountain solution class into highly forced ($-1\ll\Gamma_0<0$), weak ($\Gamma_0\lesssim-1$) and very weak fountains ($\Gamma_0\to-\infty$), and used data from experiments to show that the solution for the (initial) rise height based on the plume equations, as proposed herein, becomes invalid for very weak fountains. Comparing the source values of the rate of change of volume flux $\mathrm{d}\hat{Q}/\mathrm{d}\zeta|_{\zeta=0}=1$ (3.12*b*) and the rate of change of momentum flux $\mathrm{d}\hat{M}_B/\mathrm{d}\zeta|_{\zeta=0}=\Gamma_0$ (3.12*c*), and interpreting $\Gamma\propto(Q/M_B)^3$ as a flux balance parameter, it is evident that the momentum flux M_B approaches zero

https://doi.org/10.1017/jfm.2014.246 Published online by Cambridge University Press

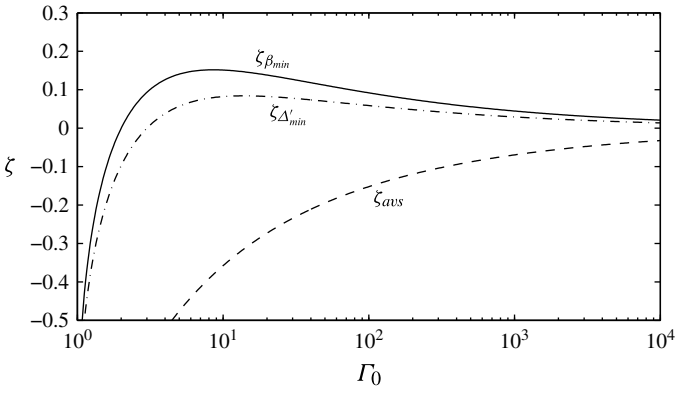

FIGURE 2. Scale diagram for planar lazy plumes showing the minimum effective half-width neck height $\zeta_{\beta_{min}}$, the maximum dilution rate height $\zeta_{\Delta'_{min}}$ and the asymptotic virtual source correction ζ_{avs}.

more rapidly for lazy fountains. Accordingly, Γ approaches $\Gamma = -\infty$ more rapidly the lazier the fountain (very negative Γ_0) and the initial rise height is smaller.

From (3.11) and (3.12), the volume flux increases monotonically with height at a monotonically decreasing rate, whereas the momentum flux decreases monotonically, but at a monotonically increasing rate, as is illustrated by figures 10(*a*,*c*) and 11(*a*,*c*). The density parameter $\hat{\Delta}$ decreases monotonically from a source value $\hat{\Delta} = 1$. The value of $\hat{\Delta}$ reached at the initial rise height, indicative of the dilution over the vertical extent of the fountain and given by taking the limit $\Gamma \to -\infty$ of (3.11), is a function of Γ_0:

$$\hat{\Delta}_{irh} = \left(\frac{\Gamma_0}{\Gamma_0 - 1}\right)^{1/3}. \tag{4.2}$$

It is evident then, that the lazier the fountain is at the source (i.e. for increasingly negative Γ_0), the larger the remaining density contrast at the initial rise height and the greater the potential role of the subsequent downflow. Thus, we may anticipate the influence of the downflow to alter depending on whether the fountain is relatively forced or relatively lazy.

Furthermore, by differentiating $\mathrm{d}\hat{w}/\mathrm{d}\zeta$ in (3.9) with respect to Γ it can be shown that the vertical acceleration reaches a maximum at a height corresponding to $\Gamma = -3$ for sufficiently forced fountains ($\Gamma_0 \geqslant -3$). For fountains that are not sufficiently forced ($\Gamma_0 < -3$) the velocity still decreases monotonically. The rate (with height) at which this decrease occurs no longer reaches a maximum but decreases monotonically with increasing distance from the source. This characteristic height denoted by $\zeta_{|w'|_{min}}$ corresponds to the maximum (negative) acceleration or, more intuitively, to the minimum deceleration and is given by substituting $\Gamma = -3$ into (3.7):

$$\zeta_{|w'|_{min}} = -\frac{1}{3}\frac{(\Gamma_0 - 1)^{1/3}}{\Gamma_0^{2/3}} \int_{\Gamma_0}^{-3} \frac{\mathrm{d}x}{x^{1/3}(x-1)^{4/3}}. \tag{4.3}$$

The minimum acceleration height thus lies between a region of rapid deceleration near the source under the influence of the undiluted effective gravity and a region near the top of the fountain where the fluid rapidly spreads in the lateral direction and the

https://doi.org/10.1017/jfm.2014.246 Published online by Cambridge University Press

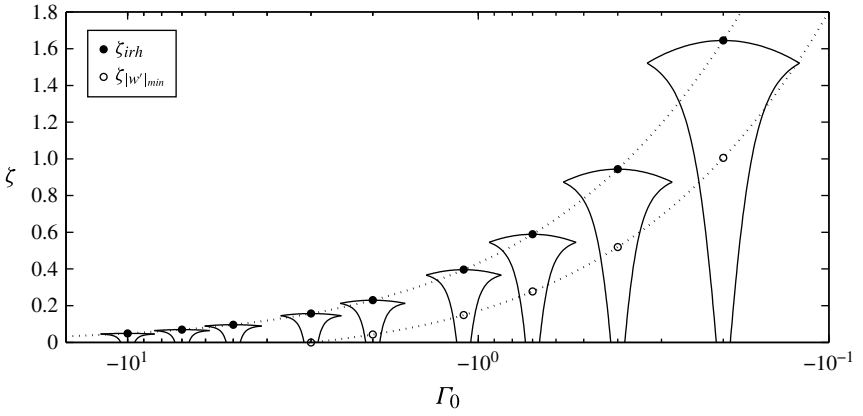

FIGURE 3. Behaviour of fountains with equivalent source half-widths b_0 as a function of Γ_0. The outline of the fountain envelope $\hat{b}(\zeta)$ is indicated. The filled circles denote the initial rise height ζ_{irh} corresponding to $\Gamma = -\infty$ and the hollow circles denote the minimum deceleration height $\zeta_{|w'|_{min}}$ corresponding to $\Gamma = -3$.

Γ	$\hat{b}$	$\hat{w}$	η	$\hat{Q}$	$\hat{G}$	$\hat{M}_B$	$\hat{M}$	$\hat{B}$
$-\infty$	∞	0	$1-(1-\eta_0)\left(\frac{\Gamma_0}{\Gamma_0-1}\right)^{1/3}$	$\left(\frac{\Gamma_0-1}{\Gamma_0}\right)^{1/3}$	$\frac{1}{\eta_0}\left(\frac{\Gamma_0-1}{\Gamma_0}\right)^{1/3}-\frac{1-\eta_0}{\eta_0}$	0	0	1

TABLE 3. Values of the quantities and fluxes for Boussinesq fountains with a constant entrainment coefficient at the initial rise height (ζ_{irh}). The form of $\hat{\Delta}_{irh}$ is given in (4.2).

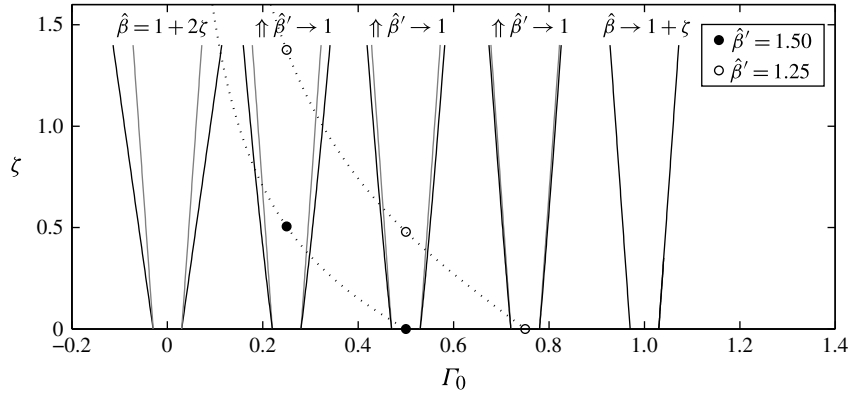

FIGURE 4. Predicted behaviour of forced plumes with equivalent effective source half-widths β_0 as a function of Γ_0 with a constant entrainment coefficient ($\kappa = 1$) (black lines and circles) and a variable entrainment coefficient ($\kappa = 1/2$) (grey lines). The filled circles denote the height at which $\mathrm{d}\hat{\beta}/\mathrm{d}\zeta = 3/2$, termed the jet-plume transition (ζ_{jpt}), the hollow circles denote the height at which $\mathrm{d}\hat{\beta}/\mathrm{d}\zeta = 5/4$. The slope converges to $\mathrm{d}\hat{\beta}/\mathrm{d}\zeta = 1$ asymptotically with height.

https://doi.org/10.1017/jfm.2014.246 Published online by Cambridge University Press

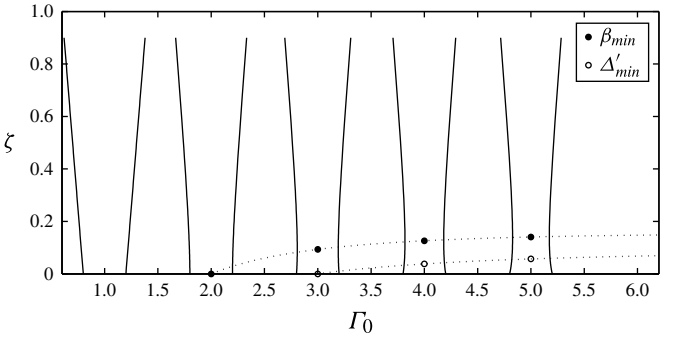

FIGURE 5. Predicted behaviour of lazy plumes with equivalent source effective half-widths β_0 as a function of Γ_0. The filled circles denote the height at which the effective half-width reaches a minimum (β_{min}) and the hollow circles denote the height at which the dilution rate reaches a maximum ($\Delta'_{min} = (\mathrm{d}\Delta/\mathrm{d}\zeta)_{min}$).

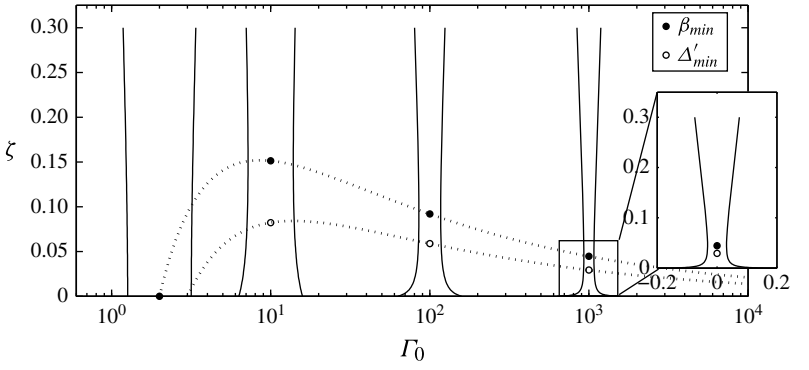

FIGURE 6. Predicted behaviour of very lazy plumes with equivalent source effective half-widths β_0 as a function of Γ_0. The filled circles denote the height at which the effective half-width reaches a minimum (β_{min}) and the hollow circles denote the height at which the dilution rate reaches a maximum ($\Delta'_{min} = (\mathrm{d}\Delta/\mathrm{d}\zeta)_{min}$).

velocity drops to conserve mass. Two regimes, gravity-driven deceleration and mixing-driven deceleration, can clearly be distinguished. It is evident from figure 8(*a*) that $\hat{\Delta}$ remains very close to its source value over a relatively large distance above the source; almost no dilution occurs in the near-source region. Additionally, the source value of the dilution rate $\mathrm{d}\hat{\Delta}/\mathrm{d}\zeta|_{\zeta=0} = -1$ (3.12*a*) does not vary with Γ_0. For relatively lazy fountains ($\Gamma_0 \leqslant -3$) the gravity-driven deceleration regime extends until the initial rise height. Only for relatively forced fountains ($\Gamma_0 \geqslant -3$) do significant mixing (cf. figure 10*a*) and dilution (cf. figure 8*a*) occur at a relatively large distance above the source (the mixing-driven deceleration regime).

4.2. *Forced plume behaviour*

For forced plumes, the characteristic heights include a height describing the transition from jet-like to plume-like behaviour (ζ_{jpt}). For a constant entrainment coefficient α the slope of the envelope of a pure jet ($\mathrm{d}\hat{\beta}/\mathrm{d}\zeta|_{\Gamma_0=0} = 2$) exceeds the slope of a pure

https://doi.org/10.1017/jfm.2014.246 Published online by Cambridge University Press

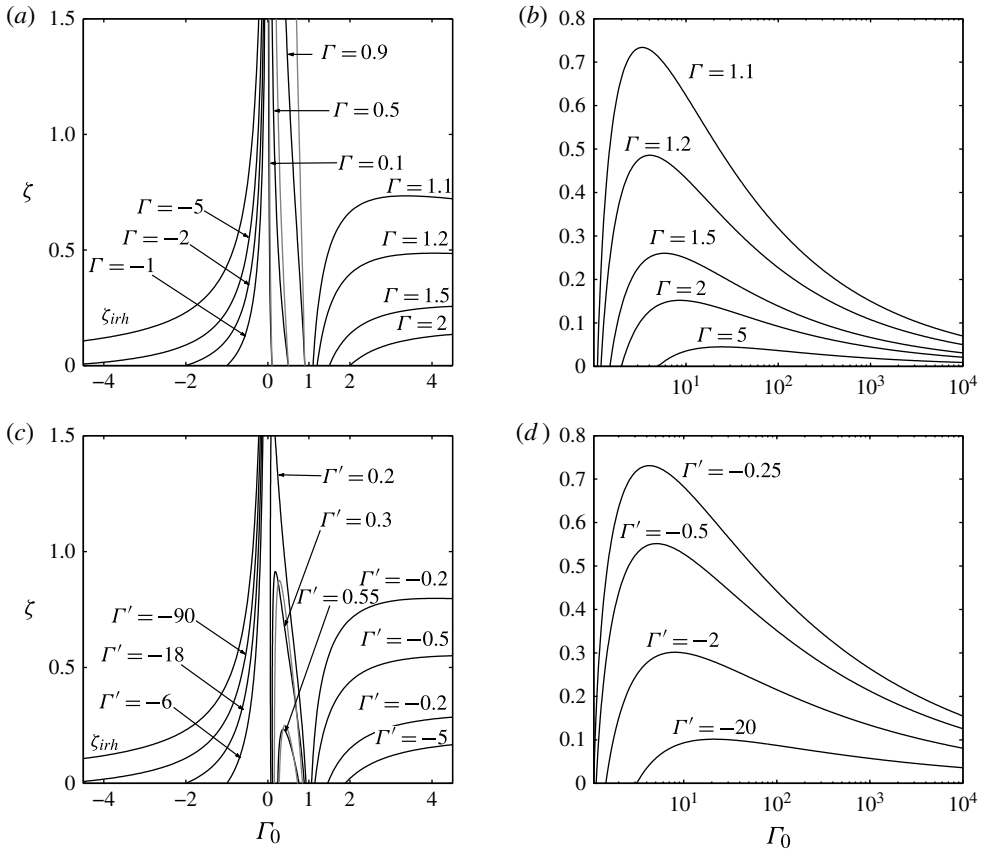

FIGURE 7. Contours of (*a*,*b*) constant Γ and (*c*,*d*) constant $\Gamma' = \mathrm{d}\Gamma/\mathrm{d}\zeta$ for releases with a constant entrainment coefficient ($\kappa = 1$) (black lines) and forced releases with a variable entrainment coefficient ($\kappa = 1/2$) (grey lines).

plume ($\mathrm{d}\hat{\beta}/\mathrm{d}\zeta|_{\Gamma_0=1} = 1$). A forced plume ($0 < \Gamma_0 < 1$) will undergo a transition from jet-like to plume-like behaviour as it rises. This transition can be characterized by a height at which the slope of the envelope is the average of a pure jet and a pure plume ($\mathrm{d}\hat{\beta}/\mathrm{d}\zeta = (1+2)/2 = 3/2$). From (2.13), it is evident that this height corresponds to $\Gamma = 1/2$. The jet–plume transition height ζ_{jpt} can be evaluated by substituting $\Gamma = 1/2$ into (3.7):

$$\zeta_{jpt} = \frac{1}{3}\frac{(1-\Gamma_0)^{1/3}}{\Gamma_0^{2/3}}\int_{\Gamma_0}^{1/2}\frac{\mathrm{d}x}{x^{1/3}(1-x)^{4/3}}, \tag{4.4}$$

and is shown as a function of Γ_0 in figure 1. We note the jet-plume transition height is defined based on the slope of the universal parameter β, which is not equal to the half-width in the non-Boussinesq case. This is discussed further in the accompanying paper (van den Bremer & Hunt 2014).

From the definition of Γ (2.12), a forced plume can be regarded as having a deficit of source volume (mass) flux or, alternatively, an excess of source momentum flux. Although both the volume (mass) flux and the momentum flux increase monotonically with height for forced plumes, it is evident from figures 10(*a*,*c*) and 11(*a*,*c*) that the

https://doi.org/10.1017/jfm.2014.246 Published online by Cambridge University Press

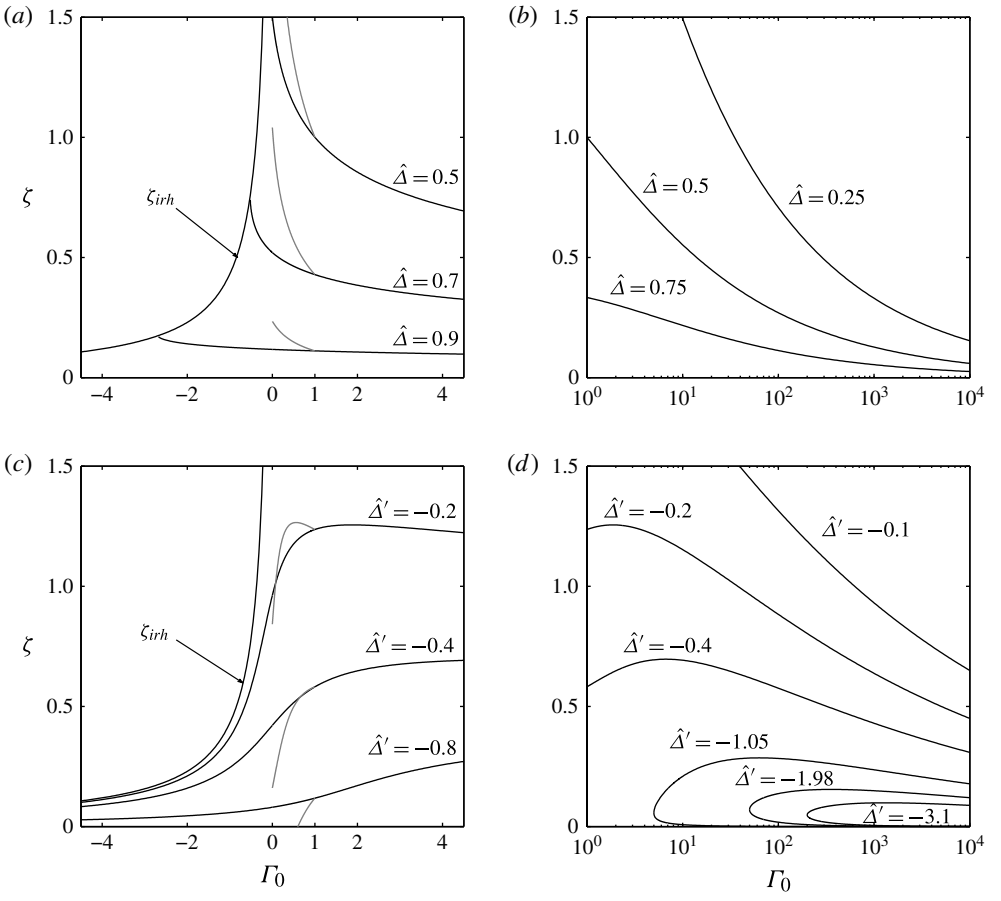

FIGURE 8. Contours of (*a*,*b*) constant $\hat{\Delta}$ and (*c*,*d*) constant $\hat{\Delta}' = \mathrm{d}\hat{\Delta}/\mathrm{d}\zeta$ for releases with a constant entrainment coefficient ($\kappa = 1$) (black lines) and forced plume releases with a variable entrainment coefficient ($\kappa = 1/2$) (grey lines).

volume (mass) flux increases generally more rapidly with height than the momentum flux. The balance of fluxes is thereby restored ($\Gamma \to 1$), and the forced plume gradually becomes pure. This adjustment is asymptotic and the pure plume limit $\Gamma \to 1$ is only reached as $\zeta \to \infty$. Note that despite the source values of the adjustment rates of the fluxes of volume (mass) and momentum ($\mathrm{d}\hat{\mathscr{G}}/\mathrm{d}\zeta|_{\zeta=0} = 1$, $\mathrm{d}\hat{\mathscr{M}}/\mathrm{d}\zeta|_{\zeta=0} = \Gamma_0$ from (3.12*b*,*c*)), the large excess of momentum flux at the source is not rapidly eroded for highly forced plumes (low Γ_0) and the adjustment to pure is very slow, achieving values of Γ close to $\Gamma = 1$ only at significant height (figure 7*a*). In fact, the flux balance adjustment relies predominantly on an increase of the volume flux due to entrainment, as the buoyancy force is relatively weak for forced plumes keeping the momentum flux more or less unchanged and, consequently, a very significant vertical extent is necessary for the work done by the buoyancy force to significantly alter the flux balance. Since the vertical velocity only decreases ($\mathrm{d}\hat{w}/\mathrm{d}\zeta|_{\zeta=0} = \Gamma_0 - 1$, see figure 9*a*,*c*), entrainment in the near-source region of forced plumes is not very significant (figure 8*a*) and significant increases in the volume flux do not occur until at a greater height (figure 10*a*).

https://doi.org/10.1017/jfm.2014.246 Published online by Cambridge University Press

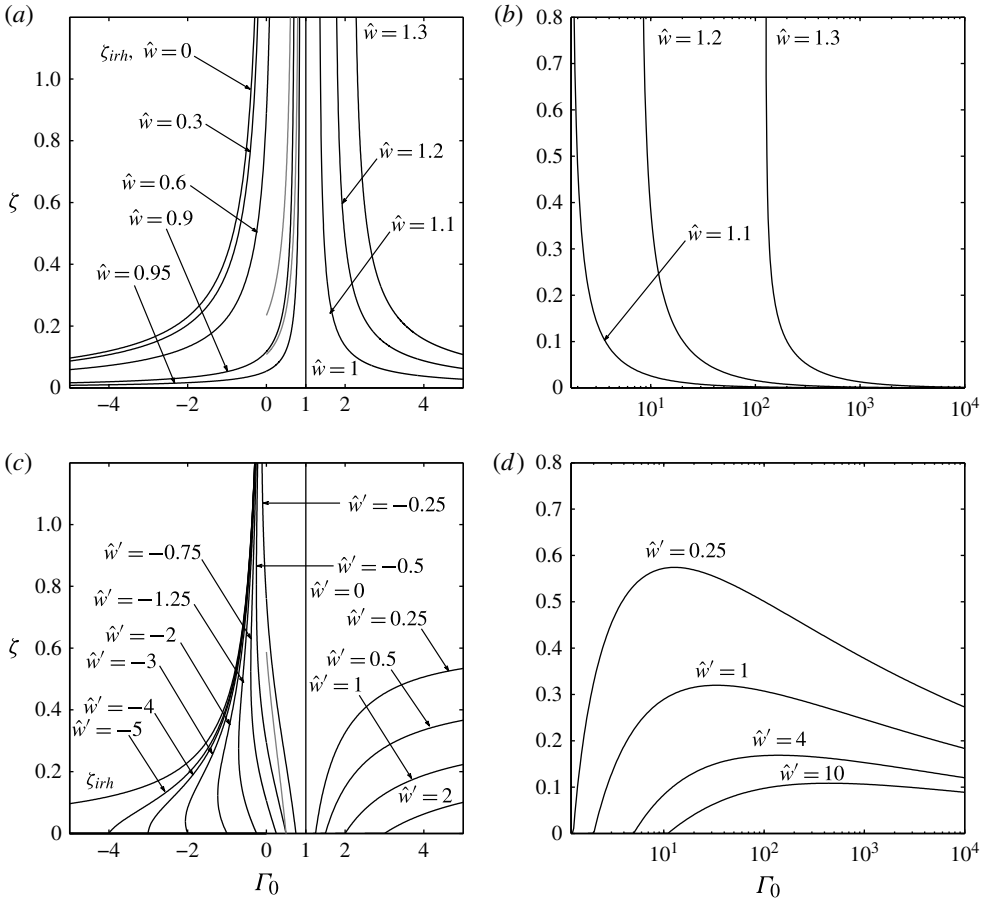

FIGURE 9. Contours of (*a*,*b*) constant $\hat{w}$ and (*c*,*d*) constant $\hat{w}' = \mathrm{d}\hat{w}/\mathrm{d}\zeta$ for releases with a constant entrainment coefficient ($\kappa = 1$) (black lines) and forced plume releases with a variable entrainment coefficient ($\kappa = 1/2$) (grey lines).

4.2.1. *Variable α (Boussinesq)*

Introducing a variable entrainment coefficient model, in which the entrainment coefficient for pure jets ($\Gamma_0 = 0$) is far smaller than for pure plumes ($\Gamma_0 = 1$), results in reduced entrainment in the near-source region of jet-like plumes. We consider the case $\kappa = 1/2$, which is in close agreement with some experimentally observed values (§ 2.3) and which corresponds to a straight-sided plume envelope. For $\kappa = 1$ the entrainment coefficient is constant. The grey lines in figures 8(*a*) and 10(*a*) clearly show the reduction in entrainment for jet-like plumes (small Γ_0). It follows from the analysis in § 3.4 and table 2 that the source value of the rate of change of momentum flux is not affected by the variable entrainment coefficient, whereas the rate of change of the volume flux and the density parameter $\hat{\Delta}$ are reduced the more jet-like the source conditions: for $\kappa = 1/2$, $\mathrm{d}\hat{Q}/\mathrm{d}\zeta|_{\zeta=0} = (1+\Gamma_0)/2$ and $\mathrm{d}\hat{\Delta}/\mathrm{d}\zeta|_{\zeta=0} = -(1+\Gamma_0)/2$ (for $\kappa = 1$, $\mathrm{d}\hat{Q}/\mathrm{d}\zeta|_{\zeta=0} = 1$ and $\mathrm{d}\hat{\Delta}/\mathrm{d}\zeta|_{\zeta=0} = -1$). Generally, the effects of $\kappa(=1/2)$ on the momentum flux are negligible (figure 11*a*,*c* in which the black and grey lines

https://doi.org/10.1017/jfm.2014.246 Published online by Cambridge University Press

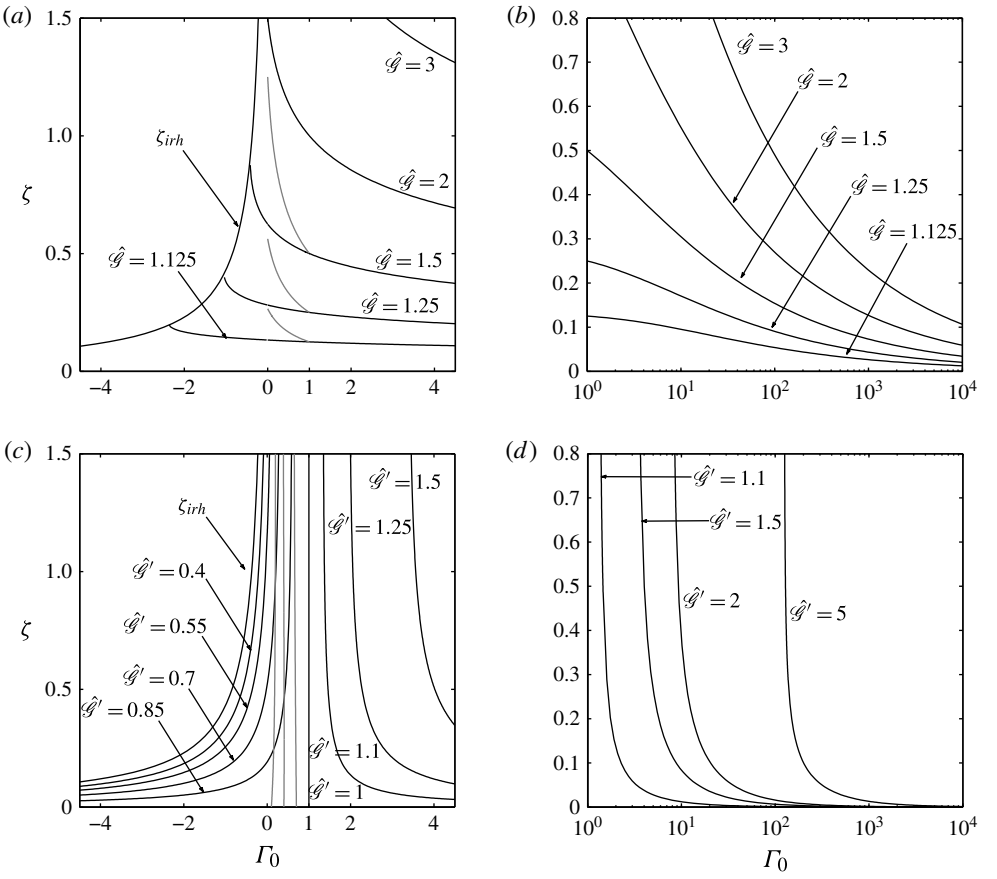

FIGURE 10. Contours of (*a*,*b*) constant $\hat{\mathscr{G}}$ and (*c*,*d*) constant $\hat{\mathscr{G}}' = \mathrm{d}\hat{\mathscr{G}}/\mathrm{d}\zeta$ for releases with a constant entrainment coefficient ($\kappa = 1$) (black lines) and forced plume releases with a variable entrainment coefficient ($\kappa = 1/2$) (grey lines).

are close to indiscernible). As a result, the volume flux deficit adjusts less rapidly and the convergence to pure plume behaviour with height is slowed (figure 7*a*).

Whereas plumes with a constant entrainment coefficient showed a less steep envelope (larger $\mathrm{d}\hat{b}/\mathrm{d}\zeta$) for small Γ_0, plumes with a variable entrainment coefficient and $\kappa = 1/2$ are straight-sided, i.e. have a (constant) slope $\mathrm{d}\hat{b}/\mathrm{d}\zeta = 1$ (figure 4 and § 3.5). As a result, jet-like forced plumes ($\Gamma_0 \approx 0$) are predicted to be steeper by a model in which the entrainment coefficient varies and $\kappa = 1/2$ (cf. figure 4). To understand how the steeper slope results from reduced entrainment, consider the rate of increase of volume flux $\hat{Q} = \hat{b}\hat{w}$, which can be written as a total derivative:

$$\frac{\mathrm{d}\hat{Q}}{\mathrm{d}\zeta} = \hat{w}\frac{\mathrm{d}\hat{b}}{\mathrm{d}\zeta} + \hat{b}\frac{\mathrm{d}\hat{w}}{\mathrm{d}\zeta}. \tag{4.5}$$

Significantly reduced entrainment (lower $\mathrm{d}\hat{Q}/\mathrm{d}\zeta$), despite marginally reduced deceleration in line with negligible changes to the momentum fluxes (cf. figure 11*a*), results in a significant reduction in the slope of the plume envelope $\mathrm{d}\hat{b}/\mathrm{d}\zeta$; the plume envelope becomes narrower.

https://doi.org/10.1017/jfm.2014.246 Published online by Cambridge University Press

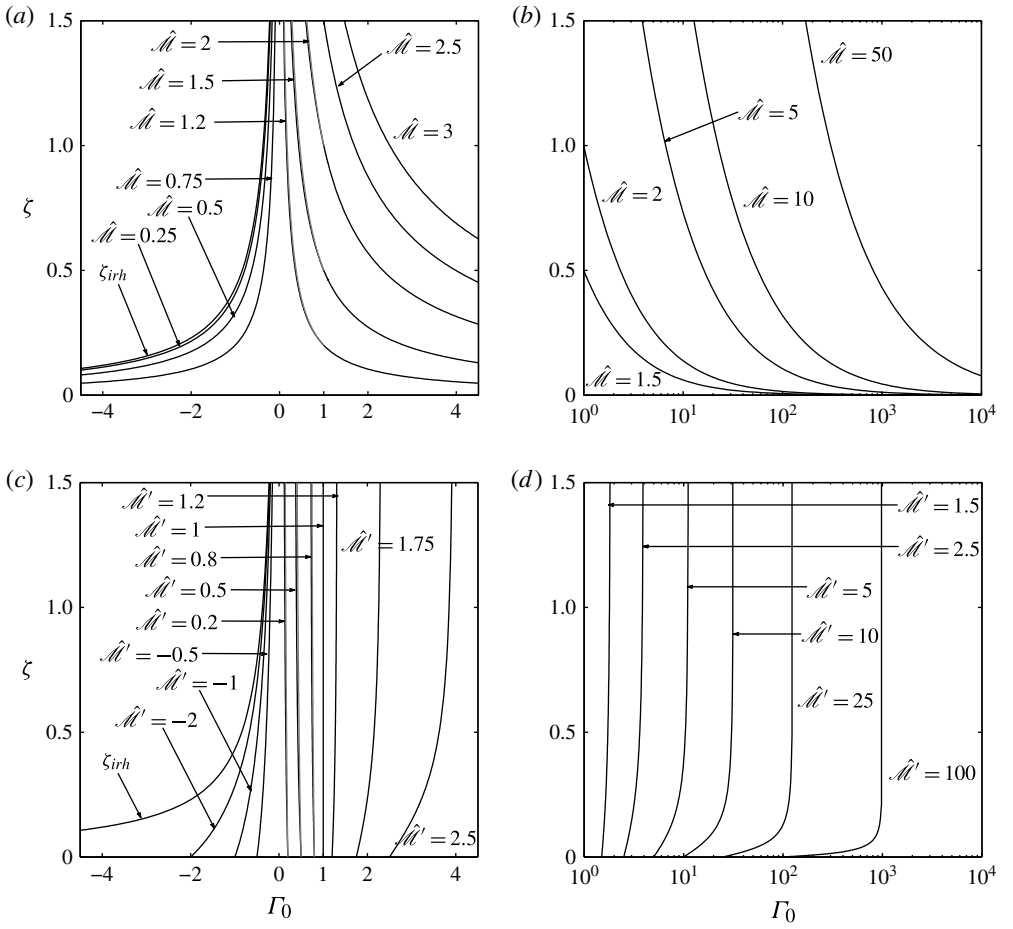

FIGURE 11. Contours of (a,b) constant $\hat{\mathscr{M}}$ and (c,d) constant $\hat{\mathscr{M}}' = \mathrm{d}\hat{\mathscr{M}}/\mathrm{d}\zeta$ for releases with a constant entrainment coefficient ($\kappa = 1$) (black lines) and forced plume releases with a variable entrainment coefficient ($\kappa = 1/2$) (grey lines).

4.3. *Lazy plume behaviour*

For lazy plumes, the characteristic heights include the height at which the effective half-width reaches a minimum ($\zeta_{\beta,min}$) and the height at which the vertical rate of change of the density parameter Δ reaches a minimum ($\zeta_{\Delta',min}$). It is evident from figure 5 that, as the lazy plume accelerates, the envelope contracts to a minimum at a relatively small distance above the source. The height at which the effective half-width of sufficiently lazy plumes ($\Gamma_0 \geqslant 2$, so that $\zeta_{\beta,min} \geqslant 0$) reaches a minimum corresponds to $\Gamma = 2$, as can be shown on differentiating (3.5) with respect to Γ or, indeed, from (2.13*b*).

In contrast to the axisymmetric case (van den Bremer & Hunt 2010), the vertical velocity does not reach a maximum at a small distance above the minimum effective half-width neck, but increases monotonically following release. Whereas in the axisymmetric case the contraction of the radius goes hand-in-hand with a vigorous reduction of the rate of volume flux increase due to entrainment, which is proportional to the radius ($\mathrm{d}\mathscr{G}/\mathrm{d}z = 2bu_e$), such a reduction is absent in the planar case. In the

https://doi.org/10.1017/jfm.2014.246 Published online by Cambridge University Press

latter case the rate of increase of the volume or mass flux does not vary with the plume effective half-width ($\mathrm{d}\mathscr{G}/\mathrm{d}z = 2u_e$). Due to the absence of this reduction in entrainment in planar plumes, sufficient ambient fluid is thereby entrained for the vertical velocity to keep increasing. It is thus a result of geometric considerations of two-dimensional versus three-dimensional plumes, that the contraction of the effective entrainment radius does entail a maximum in the vertical velocity for axisymmetric plumes, but does not for planar plumes. It is further evident from figure 9 and (3.8) that the vertical velocity decreases monotonically for forced plumes, remains constant for a pure plume and increases monotonically for lazy plumes. We note that $\zeta_{\beta,min}$ is based on the universal parameter β, which is not equal to the half-width in the non-Boussinesq case. The difference is discussed further in the accompanying paper (van den Bremer & Hunt 2014).

Figure 8(*b*,*d*) shows that the source density contrast is eroded more rapidly the lazier the plume. Despite dominance of the momentum flux relative to the volume (mass) flux in the near-source region for highly forced plumes, such plumes will maintain a greater portion of their source density contrast at any given scaled height compared to lazy plumes. For sufficiently lazy plumes ($\Gamma_0 \geqslant 3$, so that $\zeta_{\Delta',min} \geqslant 0$) the (negative) rate at which the density contrast is eroded $\Delta' = (\mathrm{d}\Delta/\mathrm{d}\zeta)$ reaches a minimum at a small distance above the source. By twice differentiating the expression for $\hat{\Delta}$ (3.11*a*) with respect to Γ, this height ($\zeta_{\Delta',min}$) can be shown to correspond to $\Gamma = 3$. In the Boussinesq case, this corresponds to the height at which $\mathrm{d}\eta/\mathrm{d}\zeta$ reaches a maximum and can therefore be interpreted as the height at which the dilution is maximal.

We recall from the definition of Γ (2.12) that a lazy plume can be regarded as having a deficit of source momentum flux or an excess of volume (mass) flux. It can be observed from figure 11(*a*,*b*) that $\mathrm{d}\hat{\mathscr{M}}/\mathrm{d}\zeta$ is greater for lazy than for forced plumes. At height, but not near the source, the same is true for $\mathrm{d}\hat{\mathscr{G}}/\mathrm{d}\zeta$ (cf. figure 10*a*,*b*), albeit with smaller differences between forced and lazy. It is clear from (3.12*c*) that the variation of the momentum flux at the source ($\mathrm{d}\hat{\mathscr{M}}/\mathrm{d}\zeta|_{\zeta=0} = \Gamma_0$) strengthens as the source departs further from that producing a pure jet. On the other hand, from (3.12*b*), the variation of the volume (mass) flux at the source $\mathrm{d}\hat{\mathscr{G}}/\mathrm{d}\zeta|_{\zeta=0} = 1$ does not respond to the value of Γ_0. As a consequence, the rate $\mathrm{d}\Gamma/\mathrm{d}\zeta$ at which the flux balance parameter is restored towards $\Gamma = 1$, the value which the plume reaches asymptotically with height, is greater for larger Γ_0. It is evident from figure 7(*b*) that for large values of Γ_0 the flux balance parameter is restored towards $\Gamma = 1$ over a relatively small height, despite the large deficit of source momentum flux. The rapid acceleration (cf. $\mathrm{d}\hat{w}/\mathrm{d}\zeta|_{\zeta=0} = \Gamma_0 - 1$, from (3.9)) and the large values of the vertical velocity that are thus reached can also explain the rapid entrainment and the maximum of $\mathrm{d}\hat{\Delta}/\mathrm{d}\zeta$, i.e. the maximum dilution rate, that is reached in the near-source region of highly lazy plumes.

5. Far-field behaviour

5.1. *Asymptotic virtual source*

For forced ($0 < \Gamma_0 < 1$) and lazy ($\Gamma_0 > 1$) plumes it is clear from (3.6) that the plume will become pure ($\Gamma \to 1$) asymptotically with height. In this far-field limit, (3.7) can be simplified (appendix E) to give:

$$\Gamma = 1 + \frac{\Gamma_0 - 1}{\Gamma_0^2}(\zeta - \zeta_{avs})^{-3}. \tag{5.1}$$

https://doi.org/10.1017/jfm.2014.246 Published online by Cambridge University Press

Equivalently, for forced plumes with a variable entrainment coefficient, the plume will become pure ($\Gamma \to 1$) asymptotically with height. In this far-field limit, (3.15) can be simplified (appendix E) to give:

$$\Gamma = 1 + \frac{\Gamma_0 - 1}{\Gamma_0^{2\kappa}}(\zeta - \zeta_{avs})^{-3\kappa}. \tag{5.2}$$

The asymptotic virtual source correction ζ_{avs} in (5.1) and (5.2) is given by (appendix E):

$$\zeta_{avs} = \begin{cases} -\dfrac{1}{\Gamma_0^{2/3}} + \dfrac{1}{3\Gamma_0^{2/3}} \displaystyle\sum_{n=1}^{n=\infty} \left(\left(\prod_{i=1}^{i=n} (i - 2/3) \right) \frac{(1-\Gamma_0)^n}{(n-1/3)n!} \right) \\ \qquad\qquad \text{for } 0 < \Gamma_0 < 1, \ \text{ constant } \alpha, \\ -\dfrac{1}{\Gamma_0^{2/3}} + \dfrac{1}{3\Gamma_0^{2/3}} \displaystyle\sum_{n=1}^{n=\infty} \left(\left(\prod_{i=1}^{i=n} (i - 2/3) \right) \frac{(1-\Gamma_0)^n}{(n\kappa-1/3)n!} \right) \\ \qquad\qquad \text{for } 0 < \Gamma_0 < 1, \ \text{ variable } \alpha, \\ -\dfrac{1}{\Gamma_0^{2/3}} + \dfrac{1}{3\Gamma_0^{2/3}} \displaystyle\sum_{n=1}^{n=\infty} \left(\left(\prod_{i=1}^{i=n} (i - 2/3) \right) \frac{\left(\frac{\Gamma_0 - 1}{\Gamma_0}\right)^n}{(n-1/3)n!} \right) \quad \text{for } \Gamma_0 > 1/2, \end{cases} \tag{5.3}$$

where we note that the domain of convergence for lazy plumes ($\Gamma_0 > 1/2$) overlaps with that for forced plumes ($0 < \Gamma_0 < 1$). We note from (5.3) that $\zeta_{avs} \to -1$ as $\Gamma_0 \to 1$, which corresponds to the origin correction for pure plumes identified in § 3.2. Furthermore, we note that the asymptotic virtual source correction for forced and lazy plumes with constant α (5.3) is equivalent to the correction obtained by Lee & Emmons (1961) using their two-step approach. For completeness, appendix D reproduces their result in the notation of this paper. By substituting the far-field expression for Γ (5.1) into (3.5), (3.8) and (3.11), the following much simplified far-field expressions for plumes with a constant entrainment coefficient are obtained respectively, to the same level of approximation:

$$\frac{\beta}{\beta_0} = \zeta - \zeta_{avs}, \quad \frac{w}{w_0} = \Gamma_0^{1/3}, \quad \frac{\Delta}{\Delta_0} = \Gamma_0^{-1/3}(\zeta - \zeta_{avs})^{-1}, \tag{5.4a–c}$$

$$\frac{\mathscr{G}}{\mathscr{G}_0} = \Gamma_0^{1/3}(\zeta - \zeta_{avs}), \quad \frac{\mathscr{M}}{\mathscr{M}_0} = \Gamma_0^{2/3}(\zeta - \zeta_{avs}). \tag{5.4d,e}$$

These far-field solutions (5.4) correspond to the solutions for pure plumes (3.3), (3.4) with an origin correction. The asymptotic virtual source correction for plumes with constant α is plotted in figure 1 as a function of Γ_0. The source conditions of a plume placed at the asymptotic virtual source that matches the original plume in the far field are summarized in table 4.

For forced plumes with a variable entrainment coefficient, the far-field solutions in (5.4) are valid without modification. It can be shown that for $\kappa = 1/2$, ζ_{avs} as defined in (5.3) reduces to $\zeta_{avs} = -1$ for any $0 < \Gamma_0 \leqslant 1$, which is in agreement with the solution for straight-sided forced plumes developed in § 3.5.

https://doi.org/10.1017/jfm.2014.246 Published online by Cambridge University Press

Γ	$\hat{w}$	$\hat{\beta}$	$\hat{\Delta}$	$\hat{\mathscr{G}}$	$\hat{\mathscr{M}}$	B/B_0
1	$\Gamma_0^{1/3}$	0	∞	0	0	1

TABLE 4. Values of the modified plume quantities and fluxes at the asymptotic virtual source (avs). The subscript 0 denotes the value at the original sources. A plume, with the source conditions in this table, placed at the asymptotic virtual source will match the original plume asymptotically with height.

5.2. *Non-Boussinesq to Boussinesq transition*

Although the far-field solutions in (5.4) as written in universal notation are directly valid for non-Boussinesq plumes, the far-field behaviour is better captured on combining the far-field solutions in (5.4) to give expressions for $\hat{b}$, $\hat{w}$ and η:

$$\frac{b}{b_0} = \xi - \xi_{avs}, \quad \frac{w}{w_0} = \Gamma_0^{1/3}, \quad \frac{1-\eta}{1-\eta_0} = \Gamma_0^{-1/3}(\xi - \xi_{avs})^{-1}. \tag{5.5a–c}$$

To aid the discussion, we have introduced in (5.5) a scaled height ξ, the definition of which does not depend on whether a Boussinesq or a non-Boussinesq model is considered:

$$\xi = \frac{\alpha z}{b_0} \quad \text{for Boussinesq and non-Boussinesq plumes.} \tag{5.7}$$

The non-Boussinesq asymptotic virtual source correction ξ_{avs} in (5.5) is given by:

$$\xi_{avs} = \eta_0 \zeta_{avs} + (1-\eta_0)\Gamma_0^{-1/3}. \tag{5.8}$$

In (5.8), ζ_{avs}, of course, depends on whether $\Gamma_0 < 1$ or $\Gamma_0 > 1$ and is given by (5.3). It is evident from (5.8), that the non-Boussinesq asymptotic virtual source correction converges to its Boussinesq equivalent in the limit $\eta_0 \to 1$. For general values of the density contrast, an additional term $(1-\eta_0)\Gamma_0^{-1/3}$ arises, the significance of which can be seen in figure 12, which plots ξ_{avs} as a function of Γ_0 for four values of η_0. Note that non-Boussinesq effects most significantly affect the asymptotic virtual source correction for relatively lazy plumes with $\Gamma_0 \sim O(10^1) - O(10^2)$.

5.3. *Non-Boussinesq to Boussinesq transition length scale*

Using the asymptotic definition of the density contrast η (5.5), the height corresponding to a specified value of η can be expressed as:

$$\xi(\Gamma_0, \eta_0, \eta) = \xi_{avs} + \Gamma_0^{-1/3}\frac{1-\eta_0}{1-\eta}, \tag{5.9}$$

where ξ_{avs} is given by (5.8). Expressing the distance from the asymptotic virtual source in (5.9) in dimensional terms enables the identification of a transition length scale measured from the asymptotic virtual source over which non-Boussinesq effects are important, namely:

$$L_{NB-B} \propto \frac{b_0}{\alpha}\Gamma_0^{-1/3}(1-\eta_0) \propto \left(\frac{B_0^2}{g^3\alpha^2}\right)^{1/3}. \tag{5.10}$$

https://doi.org/10.1017/jfm.2014.246 Published online by Cambridge University Press

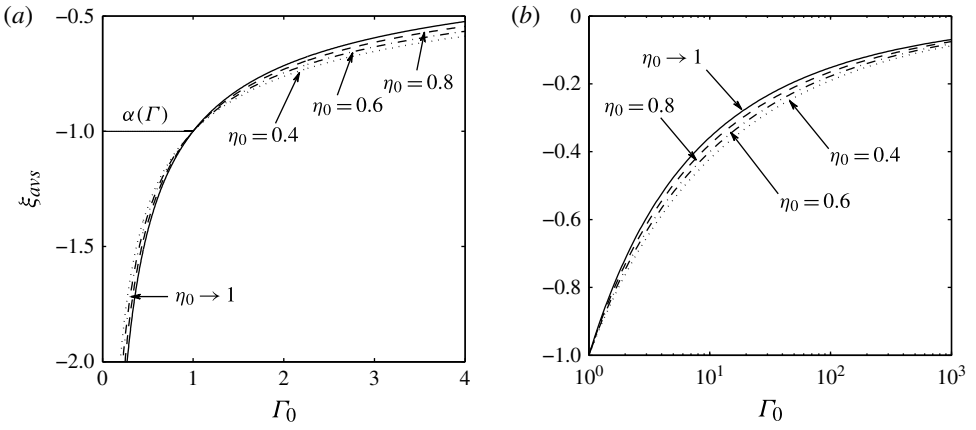

FIGURE 12. Asymptotic virtual source correction for non-Boussinesq plumes for (*a*) forced and lazy plumes and (*b*) very lazy plumes for different values of the source density contrast η_0. The horizontal line $\alpha(\Gamma)$ in (*a*) denotes the source correction $\xi_{avs} = -1$ for the entrainment model with variable α taking $\kappa = 1/2$. Note that the scaled height $\xi = \alpha z/b_0$ is independent of η_0, in contrast to the universal height $\zeta = \alpha z/\beta_0$, which is dependent on η_0 in the non-Boussinesq case $\zeta = \alpha z/b_0\eta_0 = \xi/\eta_0$, but not in the Boussinesq case $\zeta = \alpha z/b_0 = \xi$.

This is very similar to the transition length scale identified by Woods (1997) for axisymmetric plumes rising from point sources and generalized to plumes from axisymmetric area sources by van den Bremer & Hunt (2010), namely $L_{NB-B} \propto (B_0^2/g^3\alpha^4)^{1/5}$. For four different values of the source density contrast η_0, figure 13 compares, in two ways, the height that is required for the fluid to be diluted to $\eta = 0.90$ and $\eta = 0.95$, at which point we can confidently claim the plume has become Boussinesq: the numerically evaluated exact solution from (3.7) and the closed-form expression based on the far-field approximation (5.9). Figure 13 confirms that the transition length scale L_{NB-B} provides an excellent approximation to the length scale over which the transition from non-Boussinesq to Boussinesq behaviour takes place, except for very highly forced fountains. As for the axisymmetric case (cf. van den Bremer & Hunt 2010), the reason for this is that, of the two transitions that take place with height, namely $\Gamma \to 1$ and $\eta \to 1$, the former takes place more rapidly except in highly forced fountains.

6. Conclusions

Closed-form solutions to the conservation equations achieved by solving for the vertical variation of the non-dimensional flux balance parameter Γ, a local Richardson number, have been developed to describe the bulk behaviour of rising plumes and fountains from planar area sources. In doing so, we have applied the most recent findings from the literature on axisymmetric plumes to planar plumes. Despite the prevalence of planar plumes in both the man-made and the natural environment, we note that planar plumes have received remarkably little attention since the initial work by Lee & Emmons (1961) and our intention has been to bridge this gap herein. As for the axisymmetric case, the variation of Γ with height acts as a powerful instrument to describe the contrasting behaviour of releases with different source conditions: fountains ($\Gamma_0 < 0$), pure jets ($\Gamma_0 = 0$), forced plumes ($0 < \Gamma_0 < 1$), pure

https://doi.org/10.1017/jfm.2014.246 Published online by Cambridge University Press

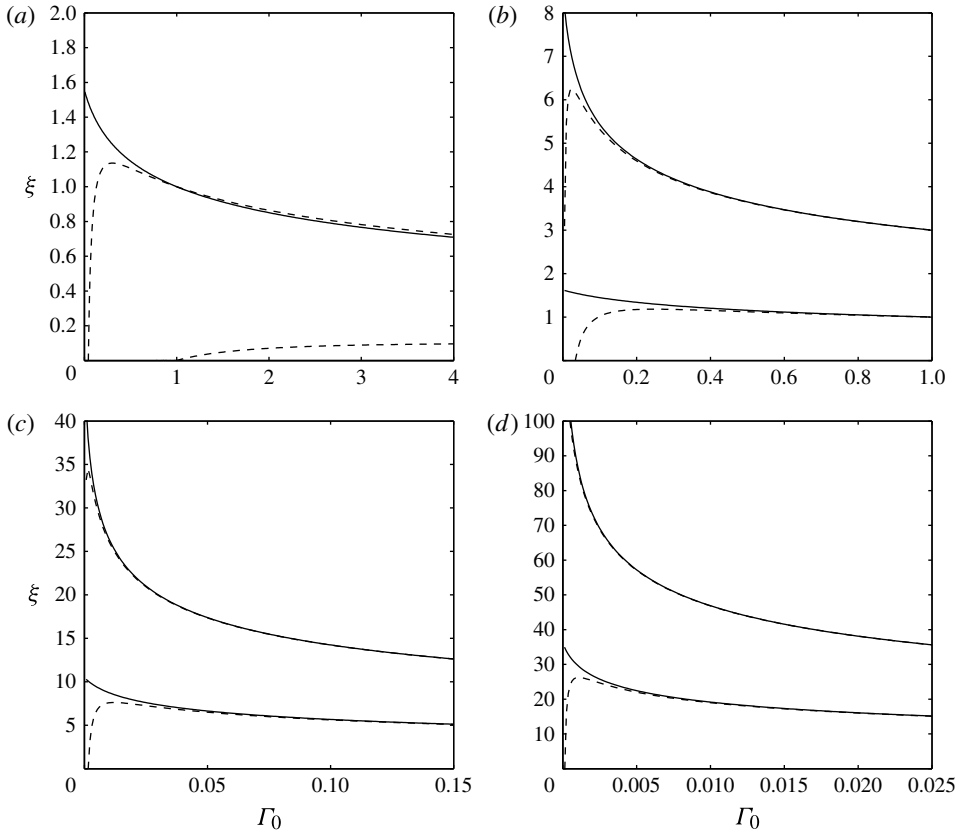

FIGURE 13. Non-Boussinesq to Boussinesq transition for (*a*) $\eta_0 = 0.9$, (*b*) $\eta_0 = 0.8$, (*c*) $\eta_0 = 0.6$, (*d*) $\eta_0 = 0.4$. Two sets of lines are plotted corresponding to $\eta = 0.95$ (upper lines) and $\eta = 0.9$ (lower lines); the continuous line corresponds to the (exact) height evaluated by numerical integration of (3.7) and the dashed line corresponds to the far-field approximation (5.9). Note that the scaled height $\xi = \alpha z/b_0$ is independent of η_0, in contrast to the universal height $\zeta = \alpha z/\beta_0$, which is dependent on η_0 in the non-Boussinesq case $\zeta = \alpha z/b_0\eta_0 = \xi/\eta_0$, but not in the Boussinesq case $\zeta = \alpha z/b_0 = \xi$.

plumes ($\Gamma_0 = 1$) and lazy plumes ($\Gamma_0 > 1$). It is exactly this contrasting behaviour that we have aimed to highlight using so-called 'scale diagrams', showing a number of non-dimensional characteristic heights as a function of a single source parameter Γ_0, first introduced by Morton & Middleton (1973) for axisymmetric plumes and generalized herein to planar plumes. Combining these scale diagrams with 'cartoons' of the actual shape or envelope of a number of representative plumes and fountains elucidates their behaviour even further. Finally, by plotting contours corresponding to constant values of some of the plume properties in (Γ_0,ζ)-space we have explored the full scope of the solutions.

Insights that have thus been gained for fountains include, but are not limited to, the identification of a gravity-driven deceleration regime and a mixing-driven regime for forced fountains, and a sole gravity-driven mixing regime for lazy fountains; and an expression for the remaining density contrast at the initial rise height of fountains, which should play a role in explaining the difference between initial and final rise heights. For plumes, these insights include a very slow convergence of highly forced

https://doi.org/10.1017/jfm.2014.246 Published online by Cambridge University Press

plumes to pure plume behaviour with height and the fact that a maximum dilution rate accompanies the necking behaviour observed in lazy plumes, but a maximum velocity is not predicted. Additionally, new solutions are found for forced Boussinesq plumes with an entrainment model in which the entrainment coefficient α varies linearly with the local Richardson number Γ, allowing for the incorporation of 'buoyancy enhanced mixing', for which experimental evidence is conclusive. For specific values of the entrainment coefficient for a pure jet and a pure plume, close to those observed, these solutions correspond to a straight-sided plume envelope.

Although there is reasonable experimental agreement between the behaviours our model predicts for pure jets and pure plumes, and this evidence is suggestive of a linear variation of the entrainment coefficient with the local Richardson number in the forced plume regime, there is no doubt that a full validation of the results herein represents a considerable undertaking and not without practical challenges. Validation of the initial rise height of planar fountains is one exception, the rise height being the principal measurement made in nearly every study of fountains (see Hunt & Coffey 2009 for a review of the data). A number of the characteristic heights identified occur in the relatively near-field region and this alone would necessitate a laboratory study using sources of a scale far exceeding those used in the works cited herein in order to adequately resolve their variation with the source conditions.

Finally, we show that if an entrainment model based on similarity is introduced for non-Boussinesq plumes, the solutions to the system of conservation equations for Boussinesq plumes and the solutions to the system of conservation equations for non-Boussinesq plumes take the same mathematical form. These 'universal solutions' rely on the introduction of an effective half-width, β, which is equal to the actual half-width, $\beta = b$, in the Boussinesq case and to the product of the half-width and the local density contrast, $\beta = b\eta$, in the non-Boussinesq case. The implications of this universality, some of which are unphysical, are discussed in an accompanying paper: van den Bremer & Hunt (2014).

Appendix A. Boussinesq conservation equations for Gaussian profiles

Adopting Gaussian profiles for the vertical velocity $w(x, z) = w_m(z)\exp(-x^2/b^2)$ and reduced gravity $g'(x, z) = g'_m(z)\exp(-x^2/b^2)$, assuming that the cross-sectional variation in both can be scaled on the same length scale b, conservation of the fluxes of volume $Q = \sqrt{\pi} w_m b$, momentum $M_B = \sqrt{\pi/2} w_m^2 b$ and buoyancy $B = \sqrt{\pi/2} w_m g'_m b$ per unit length are given by:

$$\frac{\mathrm{d}Q}{\mathrm{d}z} = 2\alpha w_m = 2^{3/2}\alpha\frac{M_B}{Q}, \quad \frac{\mathrm{d}M_B}{\mathrm{d}z} = \sqrt{\pi} g'_m b = \frac{BQ}{M_B}, \quad \frac{\mathrm{d}B}{\mathrm{d}z} = 0. \tag{A 1a–c}$$

Line-source solutions to the conservation equations with Gaussian profiles (A 1) can be found based on dimensional arguments expressing the fluxes Q and M_B as simple power-law functions of the conserved quantity B and the height z:

$$Q = 2\alpha^{2/3} B^{1/3} z, \quad M_B = 2^{1/2}\alpha^{1/3} B^{2/3} z, \tag{A 2a,b}$$

or in terms of b, w and the density parameter $\Delta = 1 - \eta$:

$$b = 2\alpha z/\sqrt{\pi}, \quad w = B^{1/3}/\alpha^{1/3}, \quad \Delta = B^{2/3}/(\alpha^{2/3}\sqrt{2} g z). \tag{A 3a–c}$$

https://doi.org/10.1017/jfm.2014.246 Published online by Cambridge University Press

The coefficients in the definition of the flux balance parameter have to be modified accordingly:

$$\Gamma = \frac{BQ^3}{2^{3/2}\alpha M_B^3} = \frac{\sqrt{\pi} g b \Delta}{\sqrt{2}\alpha w^2}. \tag{A 4}$$

By adopting the height scaling $\zeta = 2\alpha z/b_0\sqrt{\pi}$ and the modified definition of Γ in (A 4), the conservation equations for Gaussian profiles (A 1) can be shown to be equivalent to the non-dimensional conservation equations expressed in terms of Γ, ζ, $\hat{b}$ and $\hat{w}$ (2.13). Therefore, all the solutions presented herein are also valid for Boussinesq plumes with Gaussian profiles for vertical velocity and effective gravity.

Appendix B. Non-Boussinesq conservation equations for Gaussian profiles

In the solutions of Thomas & Delichatsios (2007), similarity at all horizontal sections takes the form:

$$\frac{w}{w_m} = \exp(-\hat{x}^2), \quad \frac{\rho_a - \rho}{\rho} = \left(\frac{\rho_a - \rho}{\rho}\right)_m \exp(-\hat{x}^2/\lambda^2), \tag{B 1a,b}$$

where $\hat{x}$ is a non-dimensional horizontal (cross-stream) coordinate and λ is the ratio between the w and $(\rho_a - \rho)/\rho$ profiles. Similarity can be obtained by the introduction of a stream function:

$$\Psi(x, z) = \int_0^x \frac{\rho(y)}{\rho_a} w(y) \mathrm{d}y. \tag{B 2}$$

The non-dimensional horizontal coordinate $\hat{x}$ is defined implicitly in terms of the stream function:

$$\frac{\Psi(x, z)}{\Psi(\infty, z)} = \frac{2}{\sqrt{\pi}} \int_0^{\hat{x}} \exp(-s^2) \mathrm{d}s. \tag{B 3}$$

The fluxes of mass, momentum and buoyancy are then given by:

$$G = 2\Psi(\infty, z), \quad M = \sqrt{2} w_m \Psi(\infty, z), \quad B = 2g\left(\frac{\rho_a - \rho}{\rho}\right)_m \Psi(\infty, z) \frac{\lambda}{\sqrt{1+\lambda^2}}. \tag{B 4a–c}$$

The corresponding conservation equations are, in turn, given by:

$$\frac{\mathrm{d}G}{\mathrm{d}z} = 2\alpha w_m = 2^{3/2}\alpha \frac{M}{G}, \quad \frac{\mathrm{d}M}{\mathrm{d}z} = \frac{\sqrt{1+\lambda^2}}{\sqrt{2}} \frac{BG}{M}, \quad \frac{\mathrm{d}B}{\mathrm{d}z} = 0. \tag{B 5a–c}$$

Appendix C. Universal solutions for plumes rising from line sources

Similarity solutions to the universal conservation equations (2.9) can be found by expressing $\mathscr{G}$ and $\mathscr{M}$ as power-law functions of B and z and solving for the exponents using dimensional arguments:

$$\mathscr{G} = (2\alpha)^{2/3} B^{1/3} z, \quad \mathscr{M} = (2\alpha)^{1/3} B^{2/3} z. \tag{C 1a,b}$$

The solutions in (C 1) can be combined to give:

$$\beta = \alpha z, \quad w = (2\alpha)^{-1/3} B^{1/3}, \quad \Delta = \frac{B^{2/3}}{g(2\alpha)^{2/3} z}. \tag{C 2a–c}$$

https://doi.org/10.1017/jfm.2014.246 Published online by Cambridge University Press

Equations (C 1) and (C 2) can be written entirely in universal notation by scaling on the source values of the respective quantities, denoted by the subscript 0 (and not corresponding to $z=0$ here), and combining with the definition of Γ_0 (2.12):

$$\frac{\mathscr{G}}{\mathscr{G}_0}=\Gamma_0^{1/3}\zeta, \quad \frac{\mathscr{M}}{\mathscr{M}_0}=\Gamma_0^{2/3}\zeta, \quad \frac{\beta}{\beta_0}=\zeta, \quad \frac{w}{w_0}=\Gamma_0^{1/3}, \quad \frac{\Delta}{\Delta_0}=\Gamma_0^{-1/3}\zeta^{-1}. \tag{C 3a–e}$$

Appendix D. Lee & Emmons (1961)

Taking a two-step approach, Lee & Emmons (1961) define the asymptotic virtual source correction as:

$$\zeta_{avs}=\begin{cases}-(F^2(F^2-1))^{1/3}\left(\displaystyle\int_0^{(F^2-1)^{1/3}}\frac{v}{(v^3+1)^{1/3}}\mathrm{d}v+\delta\right) & \text{for } F>1,\\ -(F^2(1-F^2))^{1/3}\left(\displaystyle\int_1^{(1-F^2)^{-1/3}}\frac{v}{(v^3-1)^{1/3}}\mathrm{d}v+\delta\right) & \text{for } 0<F<1,\end{cases} \tag{D 1}$$

where $F=\Gamma_0^{-1/2}$ is the (normalized) source Froude number. Therefore, the range $F>1$ corresponds to a forced plume ($0<\Gamma_0<1$), and the range $0<F<1$ to a lazy plume ($\Gamma_0>1$). The constant $\delta\approx 0.69$ is not evaluated explicitly in Lee & Emmons (1961), but for both forced and lazy plumes is given by:

$$\delta=1-\frac{1}{3}\sum_{n=1}^{n=\infty}\left(\prod_{i=1}^{i=n}(i-2/3)\frac{1}{(n-1/3)n!}\right). \tag{D 2}$$

Appendix E. Asymptotic virtual source correction

E.1. *Forced plumes with constant* α

The plume integral for forced plumes is given by:

$$P(\Gamma)=\int_{\Gamma_0}^{\Gamma}\frac{\mathrm{d}\Gamma}{\Gamma^{1/3}(1-\Gamma)^{4/3}}. \tag{E 1}$$

A suitable substitution is $\phi=1-\Gamma$, for which $\phi\to 0$ as $\Gamma\to 1$. Substituting for ϕ into (E 1) gives:

$$P(\phi)=-\int_{\phi_0}^{\phi}\frac{\mathrm{d}\phi}{(1-\phi)^{1/3}\phi^{4/3}}. \tag{E 2}$$

The $(1-\phi)^{-1/3}$ term in (E 2) can be expressed as a Taylor series about $\phi=0$:

$$\frac{1}{(1-\phi)^{1/3}}=1+\sum_{n=1}^{n=\infty}\left(\left(\prod_{i=1}^{i=n}(i-2/3)\right)\frac{\phi^n}{n!}\right), \tag{E 3}$$

which is valid for $0<\Gamma\leqslant 1$. Substituting (E 3) into (E 2) and integrating term by term gives:

$$P(\phi)=\left[3\phi^{-1/3}-\sum_{n=1}^{n=\infty}\left(\left(\prod_{i=1}^{i=n}(i-2/3)\right)\frac{\phi^{n-1/3}}{(n-1/3)n!}\right)\right]_{\phi_0}^{\phi}. \tag{E 4}$$

https://doi.org/10.1017/jfm.2014.246 Published online by Cambridge University Press

Taking the leading-order term in $(1-\Gamma)$ as a far-field approximation gives Γ as a function of the non-dimensional height ζ:

$$\Gamma = 1 - \frac{(1-\Gamma_0)}{\Gamma_0^2}(\zeta - \zeta_{avs})^{-3}, \tag{E 5}$$

where ζ_{avs} is the asymptotic virtual source correction:

$$\zeta_{avs} = -\frac{1}{\Gamma_0^{2/3}} + \frac{1}{3\Gamma_0^{2/3}} \sum_{n=1}^{n=\infty} \left(\left(\prod_{i=1}^{i=n} (i - 2/3) \right) \frac{(1-\Gamma_0)^n}{(n-1/3)n!} \right). \tag{E 6}$$

E.2. *Forced plumes with variable* α

The plume integral for forced plumes with an entrainment model in which α varies with Γ (2.8) is given by:

$$P(\Gamma) = \int_{\Gamma_0}^{\Gamma} \frac{\mathrm{d}\Gamma}{\Gamma^{1/3}(1-\Gamma)^{1+(1/(3\kappa))}}. \tag{E 7}$$

A suitable substitution is $\phi = 1 - \Gamma$, for which $\phi \to 0$ as $\Gamma \to 1$. Substituting for ϕ into (E 7) gives:

$$P(\phi) = -\int_{\phi_0}^{\phi} \frac{\mathrm{d}\phi}{(1-\phi)^{1/3}\phi^{1+(1/(3\kappa))}}. \tag{E 8}$$

The $(1-\phi)^{-1/3}$ term in (E 8) can be expressed as the Taylor series about $\phi = 0$ in (E 3), which is valid for $0 < \Gamma \leqslant 1$. Substituting (E 3) into (E 8) and integrating term by term gives:

$$P(\phi) = \left[3\kappa\phi^{-1/(3\kappa)} - \sum_{n=1}^{n=\infty} \left(\left(\prod_{i=1}^{i=n} (i - 2/3) \right) \frac{\phi^{n-(1/3\kappa)}}{(n-(1/3\kappa))\, n!} \right) \right]_{\phi_0}^{\phi}. \tag{E 9}$$

Taking the leading-order term in $(1-\Gamma)$ as a far-field approximation gives Γ as a function of the non-dimensional height ζ:

$$\Gamma = 1 - \frac{(1-\Gamma_0)}{\Gamma_0^{2\kappa}}(\zeta - \zeta_{avs})^{-3\kappa}, \tag{E 10}$$

where ζ_{avs} is the asymptotic virtual source correction:

$$\zeta_{avs} = -\frac{1}{\Gamma_0^{2/3}} + \frac{1}{3\Gamma_0^{2/3}} \sum_{n=1}^{n=\infty} \left(\left(\prod_{i=1}^{i=n} (i - 2/3) \right) \frac{(1-\Gamma_0)^n}{(n\kappa-1/3)n!} \right). \tag{E 11}$$

E.3. *Lazy plumes*

The plume integral for lazy plumes is given by:

$$P(\Gamma) = -\int_{\Gamma_0}^{\Gamma} \frac{\mathrm{d}\Gamma}{\Gamma^{1/3}(\Gamma-1)^{4/3}}. \tag{E 12}$$

https://doi.org/10.1017/jfm.2014.246 Published online by Cambridge University Press

A suitable substitution is $\phi = (\Gamma - 1)/\Gamma$, for which $\phi \to 0$ as $\Gamma \to 1$. Substituting for ϕ into (E 12) gives:

$$P(\phi) = -\int_{\phi_0}^{\phi} \frac{\mathrm{d}\phi}{(1-\phi)^{1/3}\phi^{4/3}}. \tag{E 13}$$

The $(1-\phi)^{-1/3}$ term in (E 13) can be expressed as a Taylor series about $\phi = 0$:

$$\frac{1}{(1-\phi)^{1/3}} = 1 + \sum_{n=1}^{n=\infty}\left(\left(\prod_{i=1}^{i=n}(i-2/3)\right)\frac{\phi^n}{n!}\right), \tag{E 14}$$

which is valid for $\Gamma > 1/2$. Substituting (E 14) into (E 13) and integrating term by term gives:

$$P(\phi) = \left[3\phi^{-1/3} - \sum_{n=1}^{n=\infty}\left(\left(\prod_{i=1}^{i=n}(i-2/3)\right)\frac{\phi^{n-1/3}}{(n-1/3)n!}\right)\right]_{\phi_0}^{\phi}. \tag{E 15}$$

Taking the leading-order term in $(\Gamma - 1)$ as a far-field approximation gives Γ as a function of the non-dimensional height ζ:

$$\Gamma = 1 + \frac{(\Gamma_0 - 1)}{\Gamma_0^2}(\zeta - \zeta_{avs})^{-3}, \tag{E 16}$$

where ζ_{avs} is the asymptotic virtual source correction:

$$\zeta_{avs} = -\frac{1}{\Gamma_0^{2/3}} + \frac{1}{3\Gamma_0^{2/3}}\sum_{n=1}^{n=\infty}\left(\left(\prod_{i=1}^{i=n}(i-2/3)\right)\frac{\left(\dfrac{\Gamma_0 - 1}{\Gamma_0}\right)^n}{(n-1/3)n!}\right). \tag{E 17}$$

REFERENCES

ANTONIA, R. A., BROWNE, L. W. B., RAJAGOPALAN, S. & CHAMBERS, A. J. 1983 On the organized motion of a turbulent plane jet. *J. Fluid Mech.* **134**, 49–66.

VAN DEN BREMER, T. S. & HUNT, G. R. 2010 Universal solutions for Boussinesq and non-Boussinesq plumes. *J. Fluid Mech.* **644**, 165–192.

VAN DEN BREMER, T. S. & HUNT, G. R. 2014 Two-dimensional planar plumes: non-Boussinesq effects. *J. Fluid Mech.* **750**, 245–258.

BUSH, J. W. M. & WOODS, A. W. 1999 Vortex generation by line plumes in a rotating stratified fluid. *J. Fluid Mech.* **388**, 289–313.

CAMPBELL, A. N. & CARDOSO, S. S. S. 2010 Turbulent plumes with internal generation of buoyancy by chemical reaction. *J. Fluid Mech.* **655**, 122–151.

CHEN, C. J. & RODI, W. 1980 *Vertical Turbulent Buoyant Jets, A Review of Experimental Data*. Pergamon.

CHING, C. Y., FERNANDO, H. J. S. & NOH, Y. 1993 Interaction of a negatively buoyant line plume with a density interface. *Dyn. Atmos. Oceans* **19** (1), 367–388.

CONROY, D. T. & LLEWELLYN SMITH, S. G. 2008 Endothermic and exothermic chemically-reacting plumes. *J. Fluid Mech.* **612**, 291–310.

DELICHATSIOS, M. A. 1988 On the similarity of velocity and temperature profiles in strong (variable density) turbulent buoyant plumes. *Combust. Sci. Technol.* **60**, 253–266.

https://doi.org/10.1017/jfm.2014.246 Published online by Cambridge University Press

FISCHER, H. B., LIST, E. J., KOH, R. C. Y., IMBERGER, J. & BROOKS, N. H. (Eds) 1979 *Mixing in Inland and Coastal Waters*. Academic.

HUNT, G. R. & VAN DEN BREMER, T. S. 2011 Classical plume theory: 1937–2010 and beyond. *IMA J. Appl. Maths* **76** (3), 424–448.

HUNT, G. R. & COFFEY, C. J. 2009 Characterising line fountains. *J. Fluid Mech.* **623**, 317–327.

HUNT, G. R. & KAYE, N. B. 2005 Lazy plumes. *J. Fluid Mech.* **533**, 329–338.

JIRKA, G. H. 2006 Integral model for turbulent buoyant jets in unbounded stratified flows part 2: plane jet dynamics resulting from multiport diffuser jets. *Environ. Fluid Mech.* **6** (1), 43–100.

KAMINSKI, E., TAIT, S. & CARAZZO, G. 2005 Turbulent entrainment in jets with arbitrary buoyancy. *J. Fluid Mech.* **526**, 361–376.

KAY, A. 2007 Warm discharges in cold fresh water. Part 1. Line plumes in a uniform environment. *J. Fluid Mech.* **574**, 239–271.

KAYE, N. B. 2008 Turbulent plumes in stratified environments: a review of recent work. *Atmos. Ocean* **46**, 433–441.

KAYE, N. B. & HUNT, G. R. 2009 An experimental study of large area source turbulent plumes. *Intl J. Heat Fluid Flow* **30**, 1099–1105.

KAYE, N. B. & SCASE, M. M. 2011 Straight-sided solutions to classical and modified plume equations. *J. Fluid Mech.* **680**, 564–573.

KOH, R. C. Y. & BROOKS, N. H. 1975 The fluid mechanics of waste-water disposal in the ocean. *Annu. Rev. Fluid Mech.* **7**, 187–211.

KOTSOVINOS, N. E. 1975 A study of the entrainment and turbulence in a plane buoyant jet. PhD thesis, California Institute of Technology.

KOTSOVINOS, N. E. 1976 A note on the spreading rate and virtual origin of a plane turbulent jet. *J. Fluid Mech.* **77**, 305–311.

KOTSOVINOS, N. E. & LIST, E. J. 1977 Plane turbulent buoyant jets. Part 1. Integral properties. *J. Fluid Mech.* **81**, 25–44.

LEE, S.-H. & EMMONS, H. W. 1961 A study of natural convection above a line fire. *J. Fluid Mech.* **11**, 353–368.

LINDEN, P. F. 2000 Convection in the environment. In *Perspectives in Fluid Dynamics: A Collective Introduction to Current Research* (ed. G. K. Batchelor, H. K. Moffatt & M. G. Worster), Cambridge University Press.

LIST, E. J. & IMBERGER, J. 1973 Turbulent entrainment in buoyant jets and plumes. *J. Hydraul. Div. ASCE* **99**, 1461–1474.

MEHADDI, R., VAUQUELIN, O. & CANDELIER, F. 2012 Analytical solutions for turbulent Boussinesq fountains in a linearly stratified environment. *J. Fluid Mech.* **691**, 487–497.

MORTON, B. R. 1959 Forced plumes. *J. Fluid Mech.* **5**, 151–163.

MORTON, B. R. & MIDDLETON, J. 1973 Scale diagrams for forced plumes. *J. Fluid Mech.* **58**, 165–176.

MORTON, B. R., TAYLOR, G. I. & TURNER, J. S. 1956 Turbulent gravitational convection from maintained and instantaneous sources. *Proc. R. Soc. Lond.* A **234**, 1–23.

PRIESTLEY, C. H. B. & BALL, F. K. 1955 Continuous convection from an isolated source of heat. *Q. J. R. Meteorol. Soc.* **81**, 144–157.

RADOMSKI, S. 2008 Natural ventilation of enclosures driven by sources of buoyancy at different elevations. PhD thesis, Imperial College London, UK.

ROONEY, G. G. 1997 Buoyant flows from fires in enclosures. PhD thesis, University of Cambridge, UK.

ROONEY, G. G. & LINDEN, P. F. 1996 Similarity considerations for non-Boussinesq plumes in an unstratified environment. *J. Fluid Mech.* **318**, 237–250.

ROUSE, H., YIH, C. S. & HUMPHREYS, H. W. 1952 Gravitational convection from a boundary source. *Tellus* **4**, 201–210.

SCASE, M. M., CAULFIELD, C. P., DALZIEL, S. B. & HUNT, J. C. R. 2006 Time-dependent plumes and jets with decreasing source strengths. *J. Fluid Mech.* **563**, 431–461.

TAYLOR, G. I. 1945 Dynamics of a mass of hot gas rising in air. *US Atomic Energy Commission* MDDC 919. LADC 276.

https://doi.org/10.1017/jfm.2014.246 Published online by Cambridge University Press

THOMAS, P. J. & DELICHATSIOS, M. A. 2007 Notes on the similarity of turbulent buoyant fire plumes with large density variations. *Fire Safety J.* **42**, 43–50.

TURNER, J. S. 1966 Jets and plumes with negative or reversing buoyancy. *J. Fluid Mech.* **26**, 779–792.

WETTLAUFER, J. S., WORSTER, M. G. & HUPPERT, H. E. 1997 Natural convection during solidification of an alloy from above with application to the evolution of sea ice. *J. Fluid Mech.* **344**, 291–316.

WIDELL, K., FER, I. & HAUGAN, P. M. 2006 Salt release from warming sea ice. *Geophys. Res. Lett.* **33**, L12501.

WOODS, A. W. 1997 A note on non-Boussinesq plumes in an incompressible stratified environment. *J. Fluid Mech.* **345**, 347–356.

WOODS, A. W. 2010 Turbulent plumes in nature. *Annu. Rev. Fluid Mech.* **42**, 391–412.

YUAN, L. M. & COX, G. 1996 An experimental study of some fire lines. *Fire Safety J.* **27**, 123–139.

https://doi.org/10.1017/jfm.2014.246 Published online by Cambridge University Press